RESEARCH MEMORANDUM

EXPERIMENTAL STATIC AERODYNAMIC FORCES AND MOMENTS AT HIGH SUBSONIC SPEEDS ON A MISSILE MODEL DURING SIMULATED LAUNCHING FROM THE MIDSEMISPAN LOCATION OF A 45° SWEPTBACK WING-FUSELAGE-PYLON COMBINATION

By William J. Alford, Jr., and Thomas J. King, Jr.

Langley Aeronautical Laboratory
Langley Field, Va.

NATIONAL ADVISORY COMMITTEE
FOR AERONAUTICS

WASHINGTON
January 10, 1957

NACA RM L56J05

NATIONAL ADVISORY COMMITTEE FOR AERONAUTICS

RESEARCH MEMORANDUM

EXPERIMENTAL STATIC AERODYNAMIC FORCES AND MOMENTS AT HIGH SUBSONIC SPEEDS ON A MISSILE MODEL DURING SIMULATED LAUNCHING FROM THE MIDSEMISPAN LOCATION OF A 45° SWEPTBACK WING-FUSELAGE-PYLON COMBINATION

By William J. Alford, Jr., and Thomas J. King, Jr.

SUMMARY

An investigation was made at high subsonic speeds in the Langley high-speed 7- by 10-foot tunnel to determine the static aerodynamic forces and moments on a missile model during simulated launching from the midsemispan location of a 45° sweptback wing-fuselage-pylon combination. The results indicated significant variations in all the aerodynamic components with changes in chordwise location of the missile. Increasing the angle of attack caused increases in the induced effects on the missile model because of the wing-fuselage-pylon combination. Increasing the Mach number had little effect on the variations of the missile aerodynamic characteristics with angle of attack except that nonlinearities were incurred at smaller angles of attack for the higher Mach numbers. The effects of finite wing thickness on the missile characteristics, at zero angle of attack, increase with increasing Mach number. The effects of the pylon on the missile characteristics were to cause increases in the rolling-moment variation with angle of attack and a negative displacement of the pitching-moment curves at zero angle of attack. The effects of skewing the missile in the lateral direction relative to and sideslipping the missile with the wing-fuselage-pylon combination were to cause additional increments in side force at zero angle of attack. For the missile yawing moments the effects of changes in skew or sideslip angles were qualitatively as would be expected from consideration of the isolated missile characteristics, although there existed differences in the yawing-moment magnitudes.

INTRODUCTION

The National Advisory Committee for Aeronautics is conducting investigations to determine the nature and origin of the mutual interference

effects experienced by various combinations of wing-fuselage models and externally carried aerial missiles. Previous investigations (refs. 1 to 5) have shown the existence of these generally objectionable effects, and references 1 and 2 have shown that they are primarily due, at low speed, to the nonuniform flow field generated in the vicinity of the airplane. The severity of these induced effects on the force and moment characteristics of a canard missile model, at high subsonic speeds, has been reported in reference 6.

The purpose of the present paper is to present the results of an experimental investigation made at high subsonic speeds to determine the static aerodynamic forces and moments on a missile model during simulated launching from the midsemispan location of a 45° sweptback wing-fuselage combination. The effects of skewing the missile relative to and sideslipping the missile with the wing-fuselage-pylon combination and the effects of removing the pylon are included for several chordwise locations. In order to expedite publication of these data, only a limited analysis is presented.

SYMBOLS

C_N missile normal-force coefficient, $\frac{\text{Normal force}}{qS_m}$

C_m missile pitching-moment coefficient, $\frac{\text{Pitching moment}}{qS_m\bar{c}_m}$

C_Y missile side-force coefficient, $\frac{\text{Side force}}{qS_m}$

C_n missile yawing-moment coefficient, $\frac{\text{Yawing moment}}{qS_m b_m}$

C_l missile rolling-moment coefficient, $\frac{\text{Rolling moment}}{qS_m b_m}$

$C_{L,A}$ wing-fuselage lift coefficient, $\frac{\text{Lift}}{qS_A}$

q free-stream dynamic pressure, lb/sq ft

V free-stream velocity, ft/sec

S_m exposed missile wing area of two panels, 0.0167 sq ft

S_A	wing area, 2.25 sq ft
b_m	span of missile wings, 0.256 ft
b	span of wing-fuselage combination, ft
c	local wing chord of airplane model, ft
$\bar{c}_m$	mean aerodynamic chord of exposed missile wing area, 0.114 ft
$\bar{c}_A$	mean aerodynamic chord of airplane wing, 0.822 ft
c_p	chord of pylon, in.
x	chordwise distance from leading edge of local wing chord to missile center of gravity (positive rearward), ft
y	spanwise distance from fuselage center line to missile center line (positive to right), ft
z	vertical distance from wing chord plane to missile center line (positive up), ft
l_s	unsupported length of missile support sting (fig. 1), ft
α	angle of attack relative to free-stream direction, deg
β_A	angle of sideslip relative to free-stream direction, deg
β_m	angle of lateral skew of missile relative to fuselage center line, deg
M	Mach number

Subscripts:

A	airplane model
m	missile model

MODELS AND APPARATUS

The wing of the wing-fuselage combination (fig. 1) used as the test vehicle had a quarter-chord sweepback of 45°, an aspect ratio of 4.0,

a taper ratio of 0.3, and NACA 65A006 airfoil sections parallel to the fuselage center line. The fuselage (with ordinates given in table I) consisted of an ogival nose section, a cylindrical center section, and a truncated tail cone. The missile model used in this investigation employed an inline cruciform arrangement of its wing and tail, with a fuselage that consisted of an ogival nose and cylindrical aftersection, and is shown in figures 1 and 2 as part of the test setup. Details of the missile model are shown in figure 3. The pylon used in this investigation had an elliptic nose section, a flat center section, and a straight tapered trailing edge. The ordinates of the pylon are given in table II.

The missile was internally instrumented with a five-component strain-gage balance and was supported from the rear of the wing-fuselage combination by a sting that was adjustable in the longitudinal, lateral, and vertical planes. The support sting also had a pivot that allowed the missile to be skewed relative to the airplane model. The missile center line was located at the midsemispan station of the wing-fuselage combination and was translated through a range of chordwise locations. For several of the chordwise locations the pylon was removed.

TESTS

The tests were made in the Langley high-speed 7- by 10-foot tunnel at Mach numbers of 0.60, 0.80, 0.90, and 0.94 with the corresponding Reynolds number varying from 3.3×10^6 to 3.8×10^6 per foot of a typical dimension. The variation of average Reynolds number with test Mach number is presented in figure 4. All tests were made through an angle-of-attack range which was restricted by the load limit of the strain-gage balance and, therefore, varied with the loading measured for each Mach number and location of the missile. The tests were made with the missile model under the left wing of the wing-fuselage combination, and the directions of positive angles and forces and moments are as shown in figure 5. The missile model was skewed $\pm 4^\circ$ relative to the unsideslipped airplane for one series of tests, and in another series of tests the complete configuration (airplane-missile configuration) was sideslipped $\pm 4^\circ$ relative to the free-stream direction.

CORRECTIONS AND ACCURACY

Blocking corrections applied to Mach number and dynamic pressure were determined by the method of reference 7. Jet-boundary corrections applied to the angle of attack were calculated by the method of reference 8.

[redacted]

Corrections have been applied to the missile angle of attack to account for the deflection of both the main sting used to support the entire wing-fuselage-missile configuration and the missile support sting and balance (figs. 1 and 2). The variation of the corrected angle of attack of the wing-fuselage combination with reference angle of attack due to the main-support-sting deflection when under load and due to jet-boundary considerations is presented in figure 6. The variation in missile angle of attack due to the deflection of the missile sting and balance combination is presented in figure 7, and a list of the missile sting lengths for the various chordwise locations investigated is presented in table III. Because of the flexibility characteristics of the missile sting and balance combination, the missile angle of attack is slightly different from the angle of attack of the wing-fuselage combination and, hence, there is some degree of incidence between the two. A study of the deflection characteristics of the two sting-support systems indicated that the maximum angle of incidence existing between the missile and the wing-fuselage combination was approximately 1.9°. The magnitude of the angle of incidence may be determined for any chordwise location from the data presented in figure 7 and table III along with the aerodynamic force and moment data of the missile.

No corrections have been applied to the missile skew angle or to the vertical or lateral locations due to the deflections of the missile sting and balance. A calibration of these deflections has been made and the results are presented in figure 7.

A study of the missile-model strain-gage-balance calibrations and general repeatability of the test data indicated that the accuracy levels of the various force and moment coefficients are approximately as follows:

Component	Accuracy
C_N	±0.05
C_m	±.05
C_Y	±.05
C_n	±.05
C_l	±.01

RESULTS AND DISCUSSION

In analyzing the force and moment characteristics of the missile model it should be kept in mind that the missile was located beneath

the left wing of the wing-fuselage-pylon combination and that the positive direction of angles and forces and moments are as shown in figure 5.

The aerodynamic characteristics of the isolated missile model and the effects of a support used to restrain the skew-angle pivot incorporated in the missile sting (fig. 1) on the isolated missile characteristics are presented in figure 8. Although breakdown tests of the isolated missile were not obtained in the present investigation, this information may be obtained from reference 9. The aerodynamic characteristics of the missile model when in the proximity of the wing-fuselage-pylon combination, at zero sideslip, are presented as a function of angle of attack for a number of Mach numbers and longitudinal locations in figure 9. The aerodynamic forces and moments of the missile model when in the proximity of the wing-fuselage combination (pylon removed), at zero sideslip, are presented in figure 10. The aerodynamic characteristics of the missile when skewed $\pm 4^\circ$ relative to and sideslipped $\pm 4^\circ$ with the wing-fuselage-pylon combination are presented in figures 11 to 13. The lift characteristics of the isolated wing-fuselage combination are presented in figure 14 for orientation.

The results of tare tests made in the clear tunnel (wing-fuselage combination removed) to evaluate the interference effects of the lateral sting support (fig. 1) upon the isolated missile aerodynamic characteristics indicated that these interference effects were negligible for the most rearward position of the missile (corresponding to $x/c = 0.50$). The interference effects of the lateral sting support upon the wing-fuselage flow fields and their corresponding effects upon the missile characteristics have not been specifically determined. It is presumed, however, that, since the lateral sting support had negligible effect upon the missile aerodynamic characteristics in the clear tunnel, it would have even smaller effect when in the presence of the wing-fuselage combination inasmuch as it would experience a smaller effective angle of attack because of the downwash induced by the wing fuselage.

The effects of a support used to restrain the skew angle pivot incorporated in the missile sting (fig. 1) are seen from figure 8 to have little effect on the missile normal force and pitching moments except at the higher Mach numbers where some nonlinearity is incurred in the slopes of the pitching-moment curves through zero angle of attack. The effects of the support on the remaining components were negligible.

The effects of varying the chordwise location of the missile relative to the leading edge of the local wing chord when the missile was in the proximity of the wing-fuselage-pylon combination (fig. 9) were to cause significant variations in all of the aerodynamic components. For the most extreme chordwise location tested ($x/c = -1.11$ in fig. 9(i)), the missile forces and moments are the least affected by the presence of the wing-fuselage-pylon combination although they are

still influenced by its presence, since the force and moment levels have not returned to their free-stream values (fig. 8). This is consistent with the low-speed observations reported in reference 3 where the missile-model forces and moments did not tend to their free-stream levels until the model was translated 1.5 wing chord lengths ahead of the leading edge of the local wing chord.

Increasing the angle of attack (fig. 9) causes increases in the induced effects on the missile because of the wing-fuselage-pylon combination. This can be explained from references 1, 2, and 9 as being due to the increase in wing circulation strength which results in increases and expansions of the downwash and sidewash angularity fields in conjunction with changes in the nonuniform dynamic-pressure field.

Increasing the Mach number (fig. 9) had, in general, little effect on the variations of the missile aerodynamic characteristics with angle of attack, except that nonlinearities were incurred at smaller angles of attack for the higher Mach numbers. The flow-disturbance effects due to finite wing thickness increase with increasing Mach number as evidenced by the displacement of the missile force and moment curves at zero angle of attack (fig. 9). This result is in accord with theoretical predictions of the effects of Mach number on the flow-field characteristics at zero lift (ref. 10).

The effect of the pylon on the missile forces and moments is seen, from a comparison of figures 9 and 10, to occur primarily in the rolling and pitching moments for the more rearward missile locations (figs. 9(b), 9(d), 10(a), and 10(b)) in that the rolling-moment variations with angle of attack are increased considerably and the pitching moments at zero angle of attack are increased negatively. As the missile is moved forward (figs. 9(g) and 10(c)), the effects of the pylon are negligible. At all the chordwise positions investigated, the pylon had negligible effect on the remaining force and moment components which is consistent with the observations of the low-speed investigation reported in reference 3. In reference 3, surprise was expressed at the lack of pylon effect on the missile side forces and yawing moments. Caution was, therefore, advised in utilizing the low-speed information at higher speeds since it had been established by reference 11 that the pylon was capable of large induction effects on the side-force variations with angle of attack for unfinned external stores. The results of the present investigation thus appear to relax, throughout the Mach number range tested, the caution mentioned in reference 3, since it must be presumed that the position of the missile wings and fins relative to the pylon must blanket, or otherwise cancel, the lateral-flow effects due to the wing. (See ref. 10.)

The effects of skewing the missile relative to the wing-fuselage-pylon combination (figs. 11(a) and (b), 12(a) and (b), and 13(a) and (b))

and the effects of sideslipping the complete configuration (wing-fuselage-pylon-missile combination in figs. 11(c) and (d), 12(c) and (d), and 13(c) and (d)) were, in general, qualitatively similar with the most significant changes occurring in the missile side force and yawing moments. The most noteworthy effect on the side-force characteristics appears in the incremental changes at zero angle of attack with changes in the skew and sideslip angles with these increments being approximately the same as would be expected from consideration of the isolated missile characteristics (fig. 8, with the proper sign changes). For the yawing moments, the effects of varying the skew or sideslip angles are, in general, qualitatively as would be expected from consideration of the isolated missile characteristics (fig. 8, with the proper changes in the nondimensionalizing parameters and signs) in that for a given chordwise location and angle of attack a negative value of the skew or sideslip angle produces a negative increment in the yawing moment and a positive value of the angle produces a positive increment. The magnitude of the yawing-moment increments with the skew or sideslip angles is not, however, generally the same as indicated by the isolated missile aerodynamic characteristics. This is presumed due to the non-uniform flow conditions generated by the wing-fuselage combination.

CONCLUDING REMARKS

The results of an experimental investigation made at high subsonic speeds to determine the static aerodynamic forces and moments on a missile model during simulated launching from the midsemispan location of a 45° sweptback wing-fuselage combination indicate significant variations in all of the aerodynamic components with changes in chordwise location of the missile. Increasing the angle of attack caused increases in the induced effects on the missile model because of the wing-fuselage-pylon combination. Increasing the Mach number had little effect on the variation with angle of attack of the missile aerodynamic characteristics, except that nonlinearities were incurred at smaller angles of attack for the higher Mach numbers. The effects of finite wing thickness on the missile aerodynamic characteristics, at zero angle of attack, increase with increasing Mach number. The effects of the pylon on the missile characteristics were to cause increases in the rolling-moment variation with angle of attack and a negative displacement of the pitching-moment curves at zero angle of attack.

The effects of skewing the missile relative to and sideslipping the missile with the wing-fuselage-pylon combination were to cause additional increments in side force at zero angle of attack. For the missile yawing

moments, the effects of changes in skew or sideslip angles were qualitatively as would be expected from consideration of the isolated missile characteristics, although there existed differences in the yawing-moment magnitudes.

Langley Aeronautical Laboratory,
National Advisory Committee for Aeronautics,
Langley Field, Va., September 18, 1956.

REFERENCES

1. Alford, William J., Jr., Silvers, H. Norman, and King, Thomas J., Jr.: Preliminary Low-Speed Wind-Tunnel Investigation of Some Aspects of the Aerodynamic Problems Associated With Missiles Carried Externally in Positions Near Airplane Wings. NACA RM L54J20, 1954.

2. Alford, William J., Jr.: Effects of Wing-Fuselage Flow Fields on Missile Loads at Subsonic Speeds. NACA RM L55E10a, 1955.

3. Alford, William J., Jr., Silvers, H. Norman, and King, Thomas J., Jr.: Experimental Aerodynamic Forces and Moments at Low Speed of a Missile Model During Simulated Launching From the Midsemispan Location of a 45° Sweptback Wing-Fuselage Combination. NACA RM L54K11a, 1955.

4. Alford, William J., Jr.: Experimental Static Aerodynamic Forces and Moments at Low Speed on a Canard Missile During Simulated Launching From the Midsemispan and Wing-Tip Locations of a 45° Sweptback Wing-Fuselage Combination. NACA RM L55A12, 1955.

5. Alford, William J., Jr., Silvers, H. Norman, and King, Thomas J., Jr.: Experimental Static Aerodynamic Forces and Moments at Low Speed on a Missile Model During Simulated Launching From the 25-Percent-Semispan and Wing-Tip Locations of a 45° Sweptback Wing-Fuselage Combination. NACA RM L55D20, 1955.

6. Alford, William J., Jr., and King, Thomas J., Jr.: Experimental Static Aerodynamic Forces and Moments at High Subsonic Speeds on a Canard Missile During Simulated Launching From the Midsemispan Location of a 45° Sweptback Wing-Fuselage-Pylon Combination at Zero Sideslip. NACA RM L56J15a, 1956.

7. Herriot, John G.: Blockage Corrections for Three-Dimensional-Flow Closed-Throat Wind Tunnels, With Consideration of the Effect of Compressibility. NACA Rep. 955, 1950. (Supersedes NACA RM A7B28.)

8. Gillis, Clarence L., Polhamus, Edward C., and Gray, Joseph L., Jr.: Charts for Determining Jet-Boundary Corrections for Complete Models in 7- by 10-Foot Closed Rectangular Wind Tunnels. NACA WR L-123, 1945. (Formerly NACA ARR L5G31.)

9. Johnson, M. C., and Copley, R. J.: Presentation of Normal Force, Pitching Moment, and Rolling Moment Data From Wind Tunnel Tests of the 13.5-Percent-Scale Model of the Sparrow 14-B at Mach Numbers of 0.5, 0.7, and 0.8. Rep. No. SM-14334 (Contract NOa(s)51-859), Douglas Aircraft Co., Inc., Dec. 30, 1952.

10. Alford, William J., Jr.: Theoretical and Experimental Investigation of the Subsonic-Flow Fields Beneath Swept and Unswept Wings With Tables of Vortex-Induced Velocities. NACA TN 3738, 1956.

11. Guy, Lawrence D.: Loads on External Stores at Transonic and Supersonic Speeds. NACA RM L55E13b, 1955.

TABLE I.- FUSELAGE ORDINATES

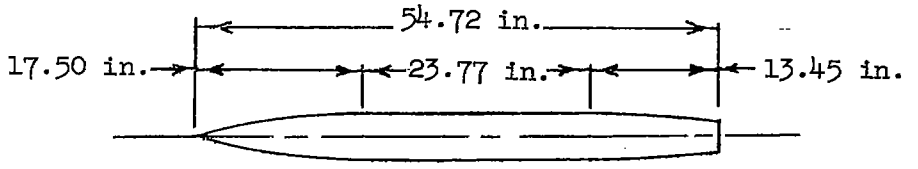

Ordinates, in.	
Station	Radius
0	0
2.00	.53
4.00	1.00
6.00	1.44
8.00	1.80
10.00	2.07
12.00	2.30
14.00	2.42
16.00	2.47
17.50	2.50
41.27	2.50
43.27	2.42
45.27	2.35
47.27	2.25
48.30	2.14
54.72	1.65

[redacted]

TABLE II.- PYLON ORDINATES

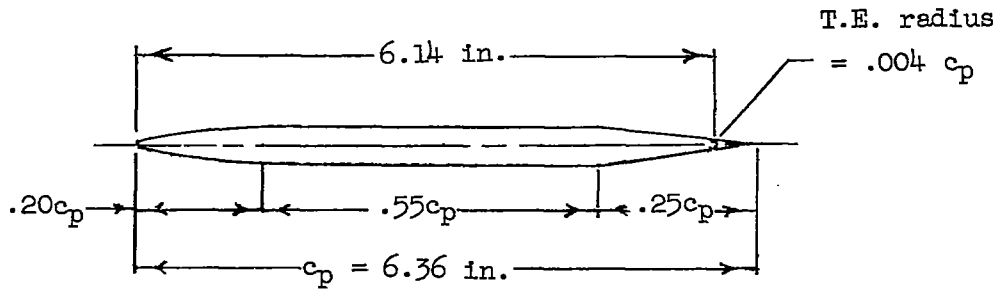

Ordinates, percent chord	
x	±y
0	0
2.5	1.45
5.0	2.00
15.0	2.90
20.0	3.00
75.0	3.00
Straight taper	
100.0	0

TABLE III.- MISSILE STING LENGTHS

Missile center-of-gravity location, x/c	Unsupported sting length, $l_s/\bar{c}_A$ (b)
(a)	1.91
0.50	1.24
.29	1.44
.13	1.58
-.10	1.79
-.25	1.01
-.44	1.08
-.58	1.31
-.74	1.35
-1.11	1.69

[a]Isolated missile.

[b]For the missile center-of-gravity locations $x/c = -0.25$ to $x/c = -1.11$, the missile sting was clamped to the pylon of the wing-fuselage-pylon combination.

[redacted]

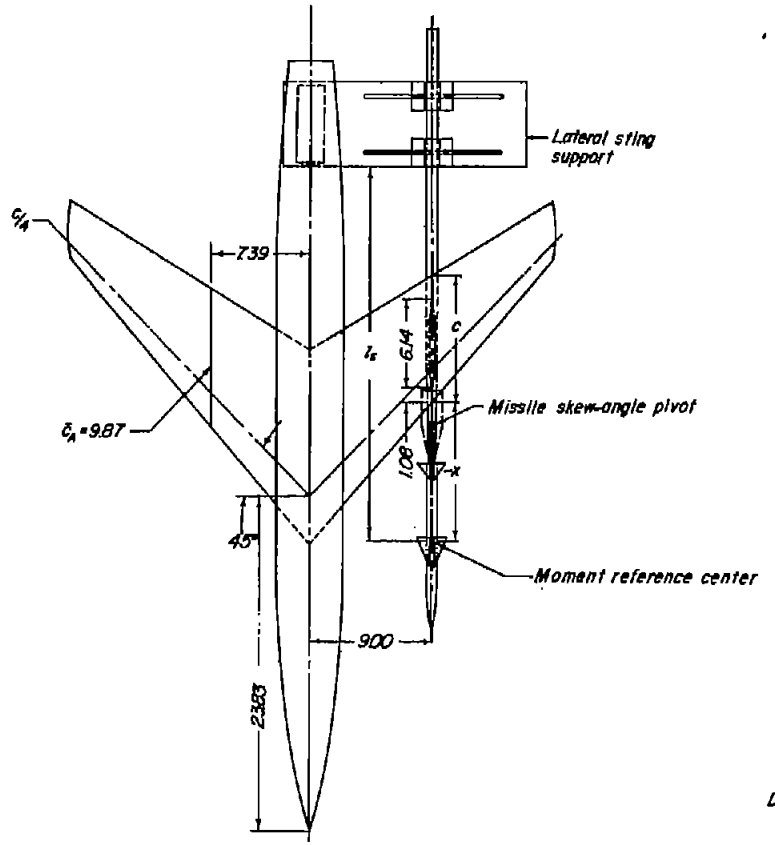

Wing Geometry Of Swept Wing-Fuselage Model

Area	2.25 sq ft
Aspect ratio	4.00
Taper ratio	0.30
Tip chord	4.15 in.
Root chord	13.85
Streamwise airfoil section	NACA 65A006

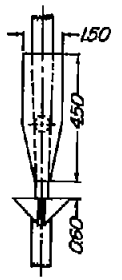

Details of skew-angle pivot support

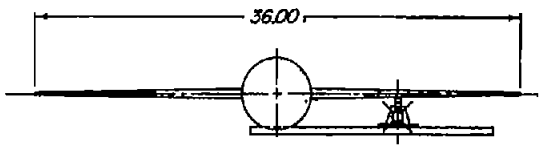

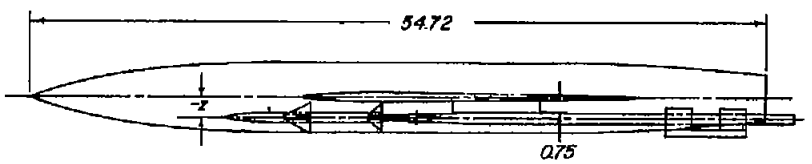

Figure 1.- Three-view drawing of wing-fuselage combination with missile model installed. All dimensions are in inches except where noted.

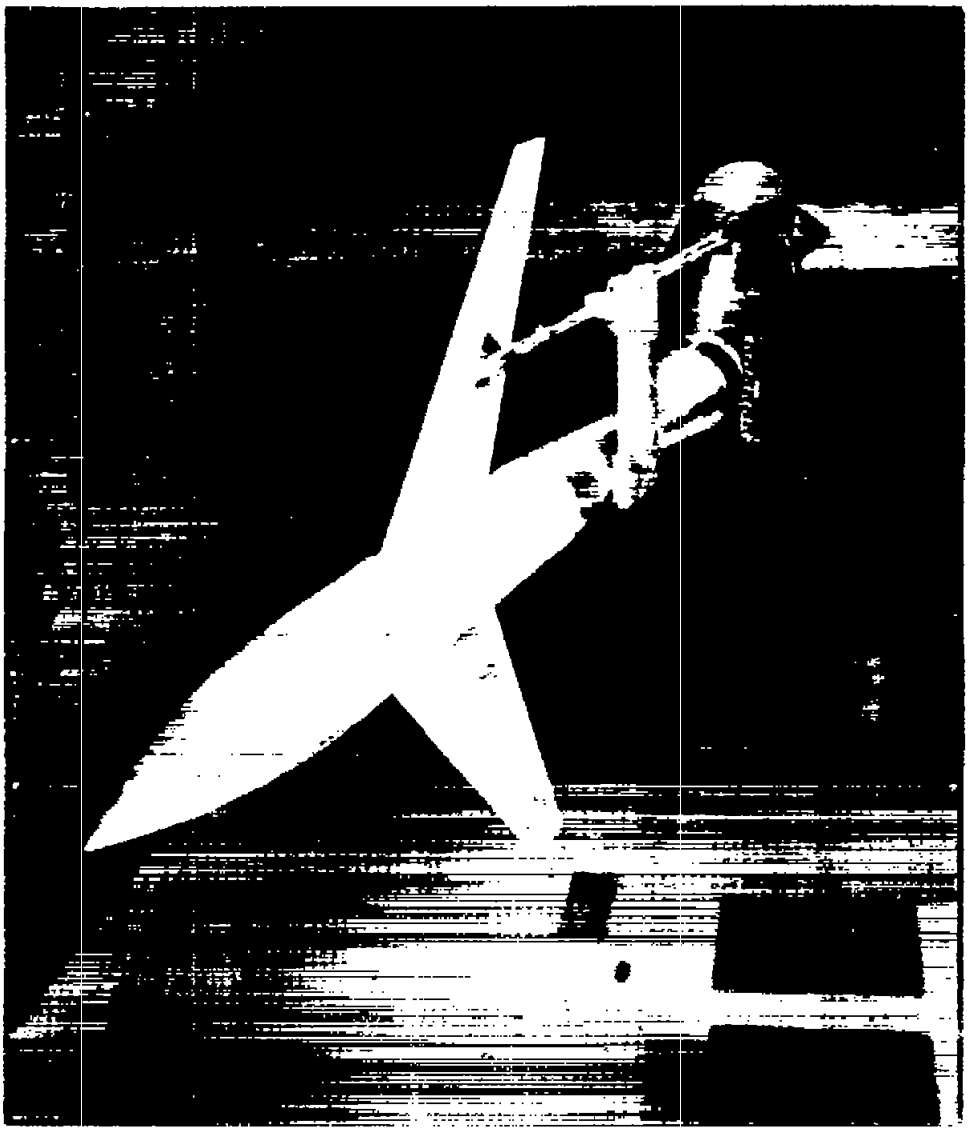

L-90313

Figure 2.- Photograph of typical test setup. (Photograph is inverted for orientation.)

[redacted]

Nose ordinates, inches	
x_m	r
0	0
.500	.082
1.000	.153
1.500	.214
2.000	.264
2.500	.302
3.000	.331
3.500	.348
4.050	.355

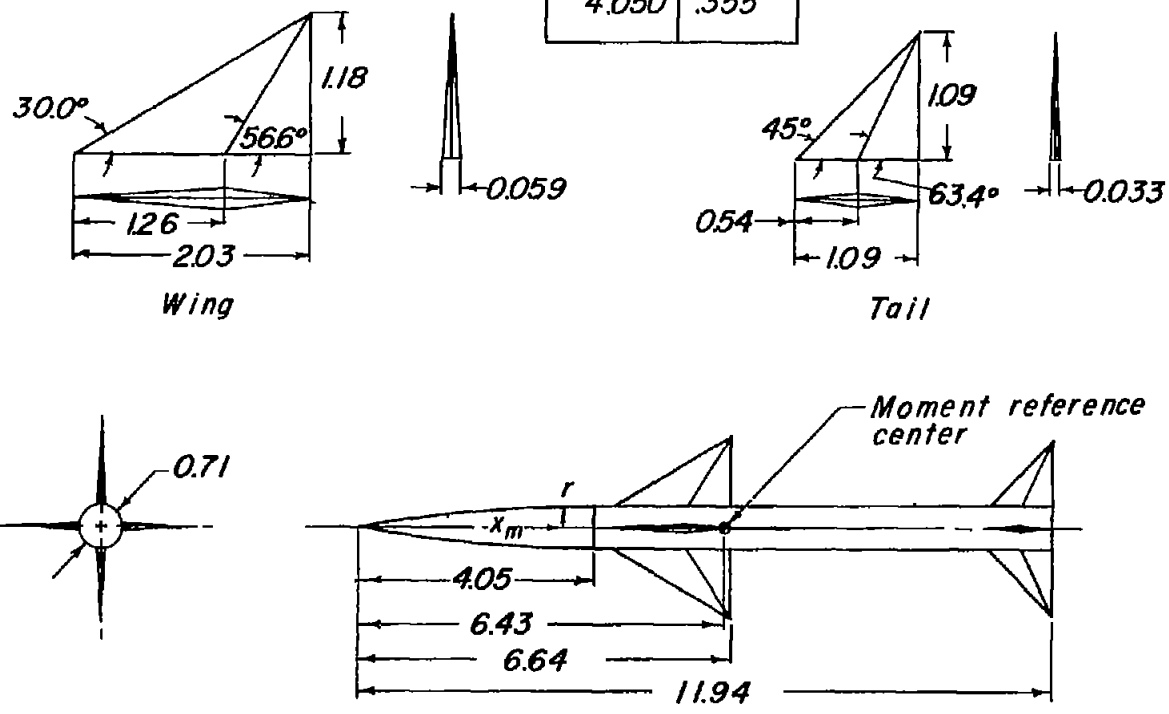

Figure 3.- Drawing of missile model. All linear dimensions are in inches.

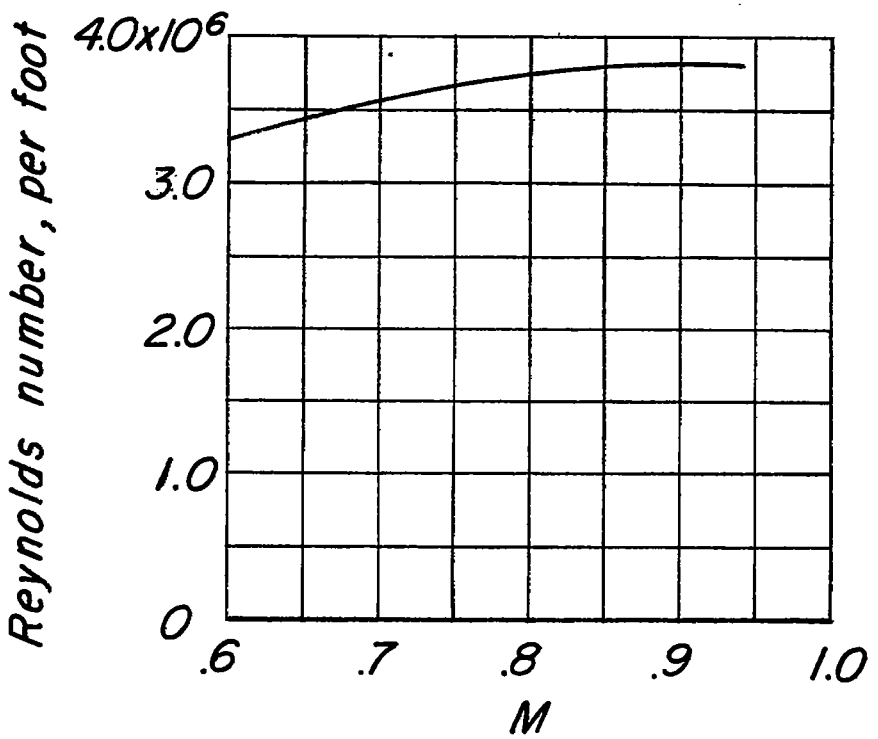

Figure 4.- Variation of average Reynolds number with test Mach number.

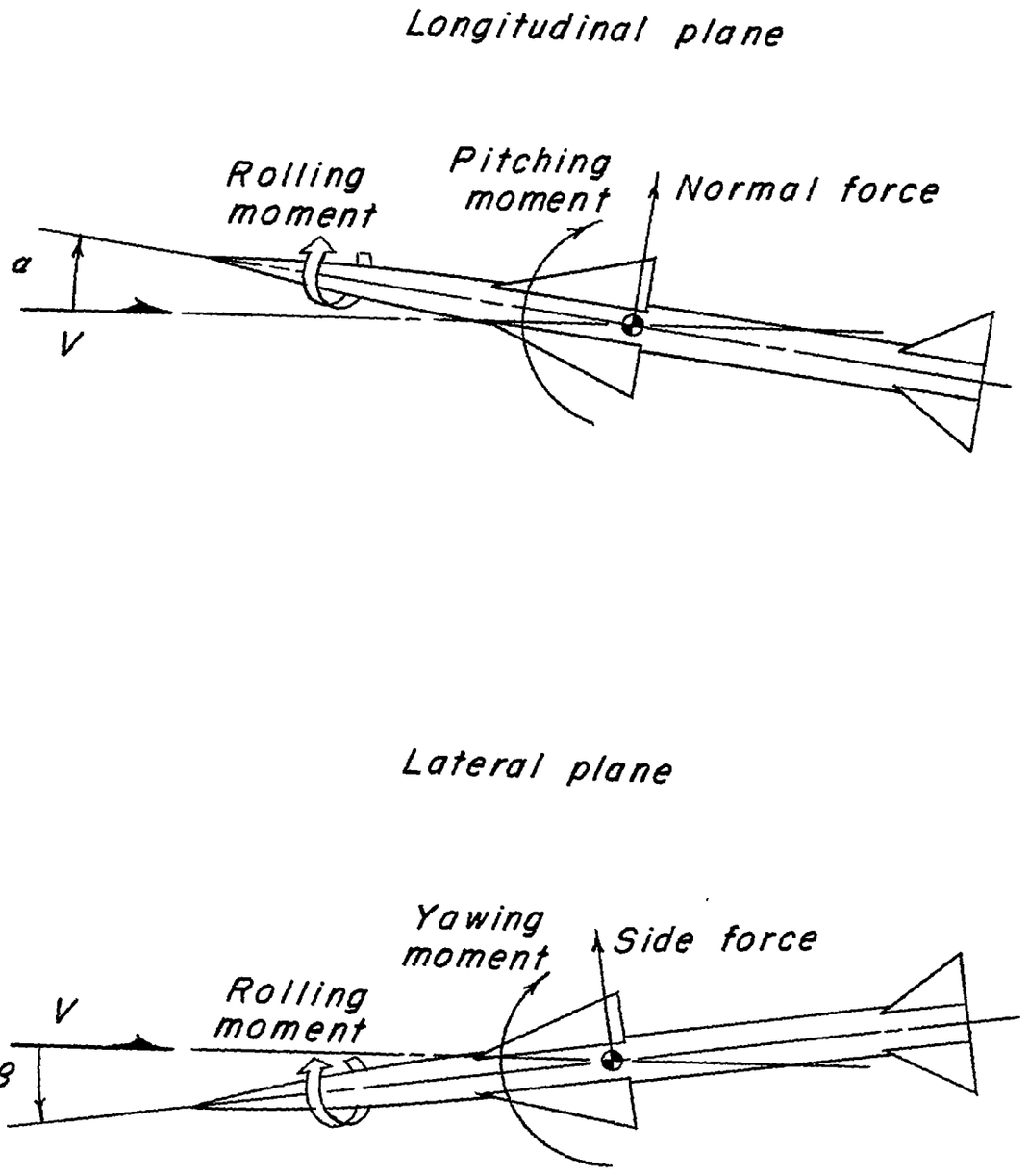

Figure 5.- Positive directions of forces and moments as measured on the missile.

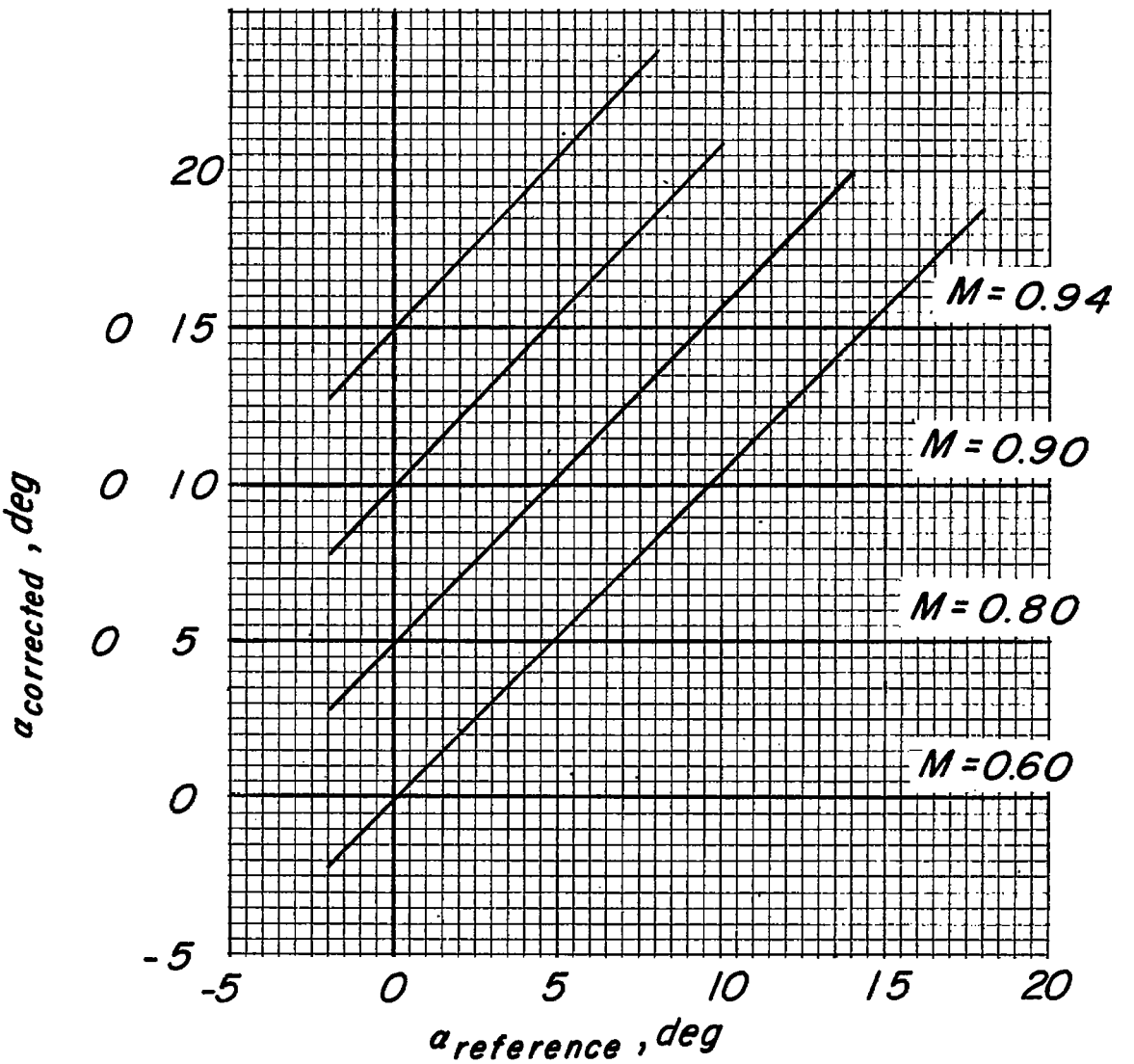

Figure 6.- Variation of corrected angle of attack of wing-fuselage model with reference angle of attack.

[redacted]

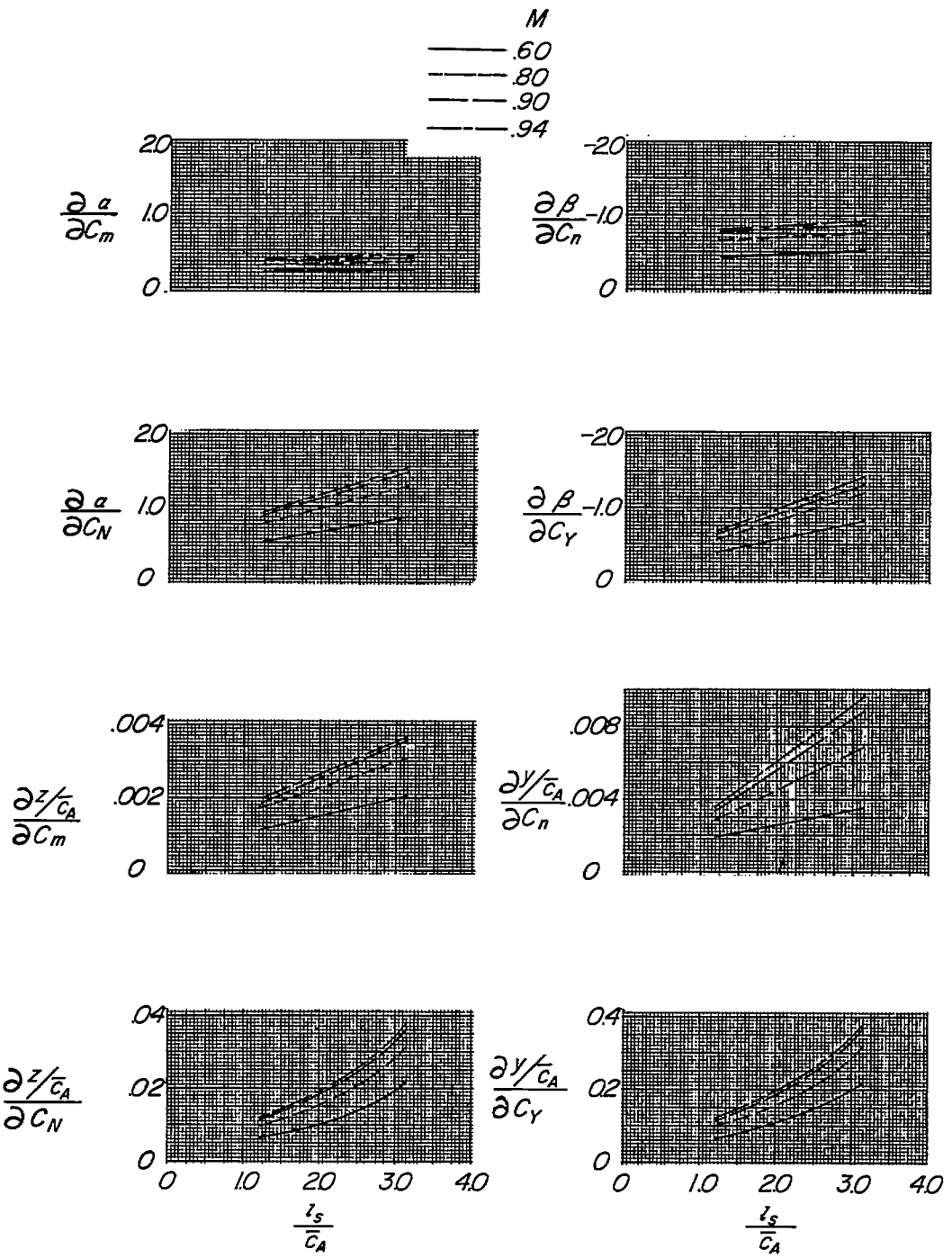

Figure 7.- Deflection characteristics of sting-balance combination. Angular deflections are in degrees.

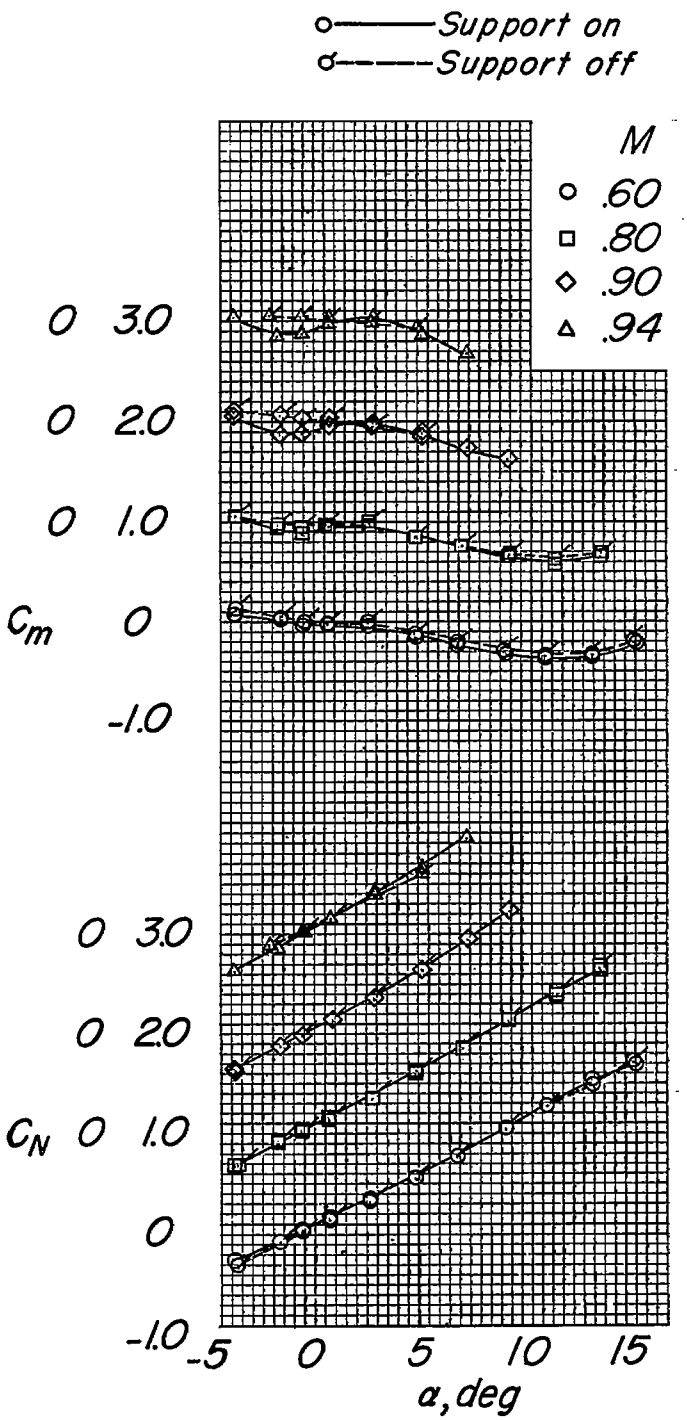

Figure 8.- Aerodynamic forces and moments of the isolated missile.

[redacted]

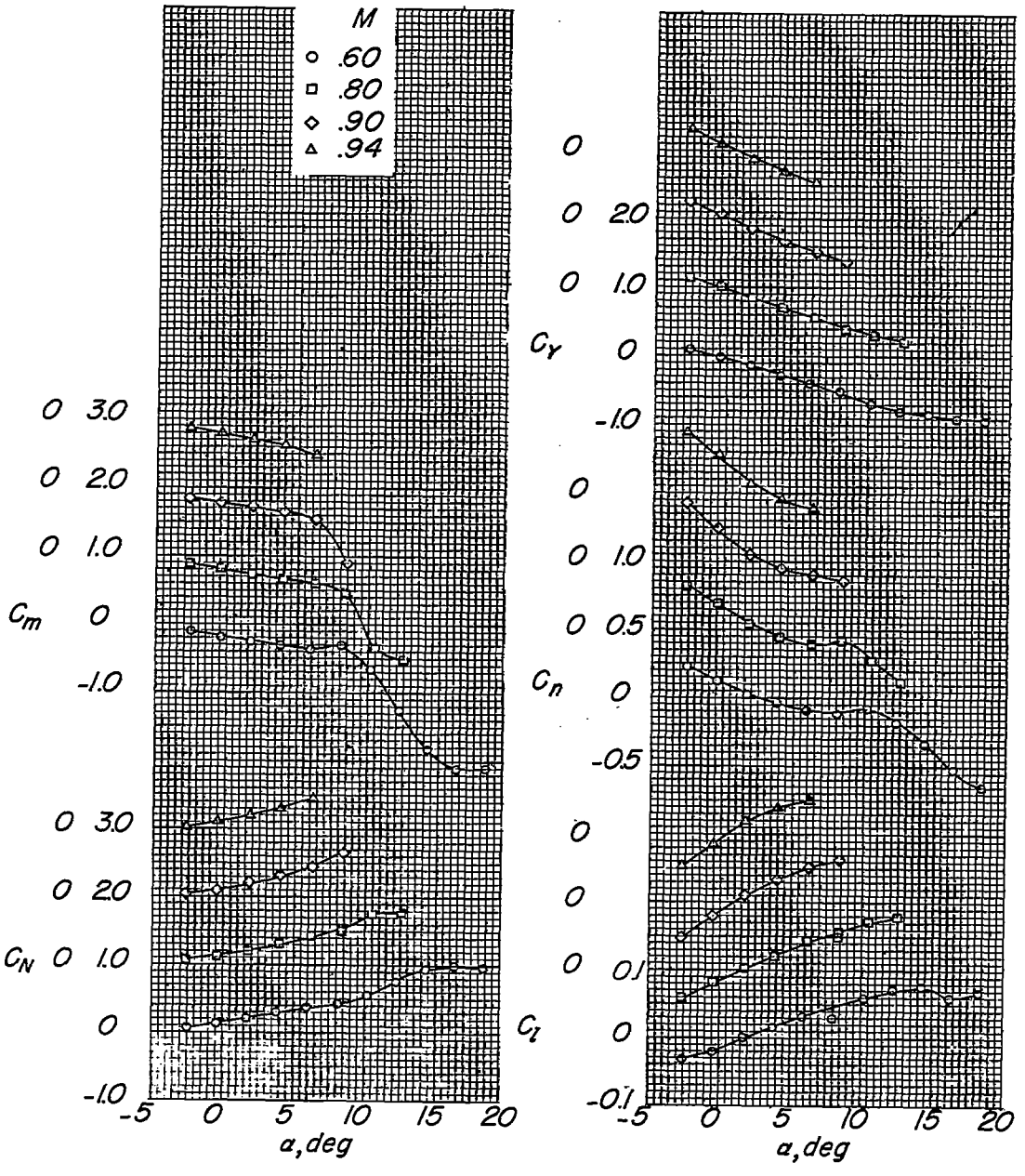

(a) x/c = 0.50.

Figure 9.- Missile aerodynamic forces and moments in the presence of the wing-fuselage-pylon combination for various Mach numbers and chordwise locations. z/c = -0.16; $\beta_m = 0^\circ$; $\beta_A = 0^\circ$.

[redacted]

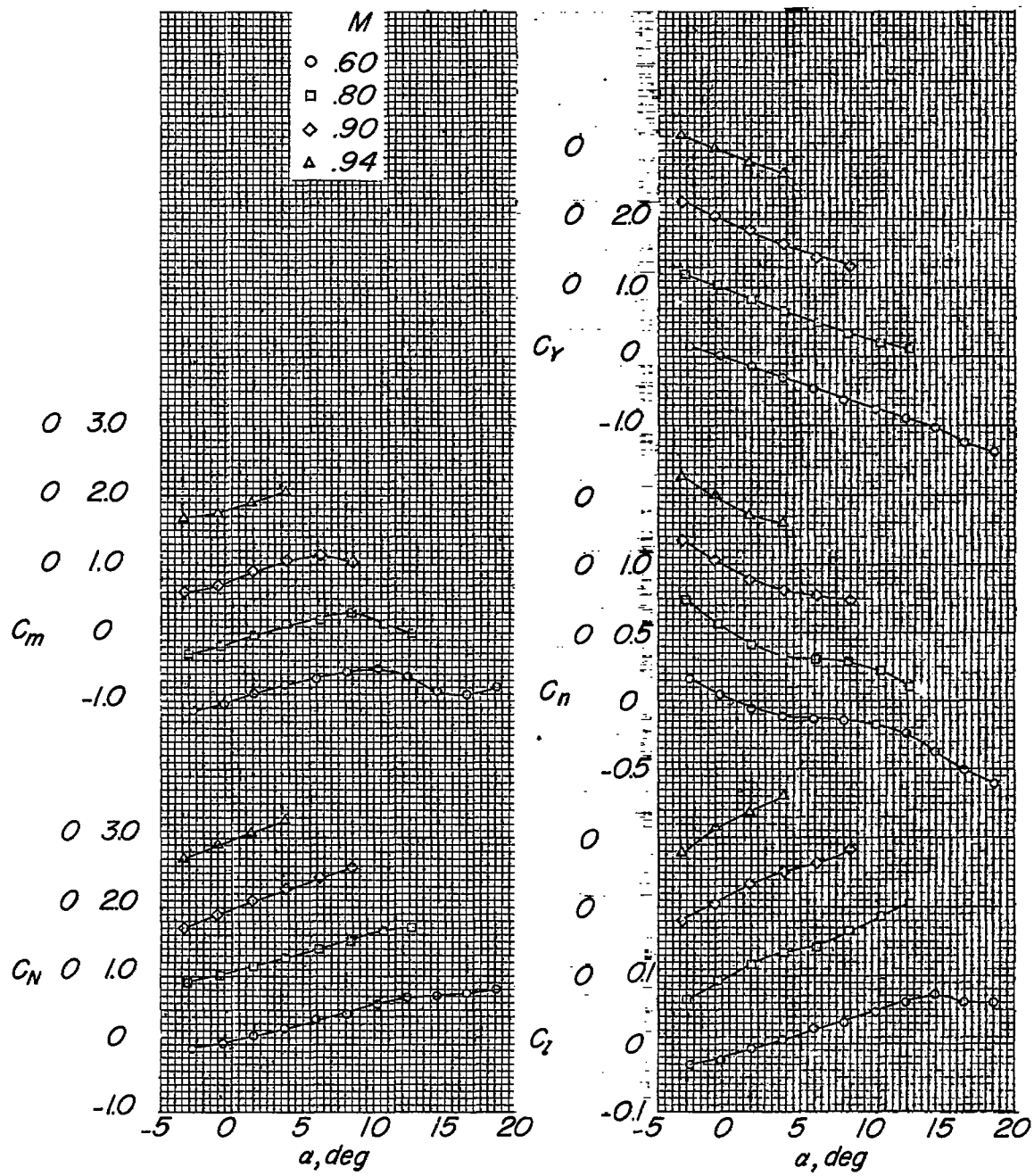

(b) x/c = 0.29.

Figure 9.- Continued.

[redacted]

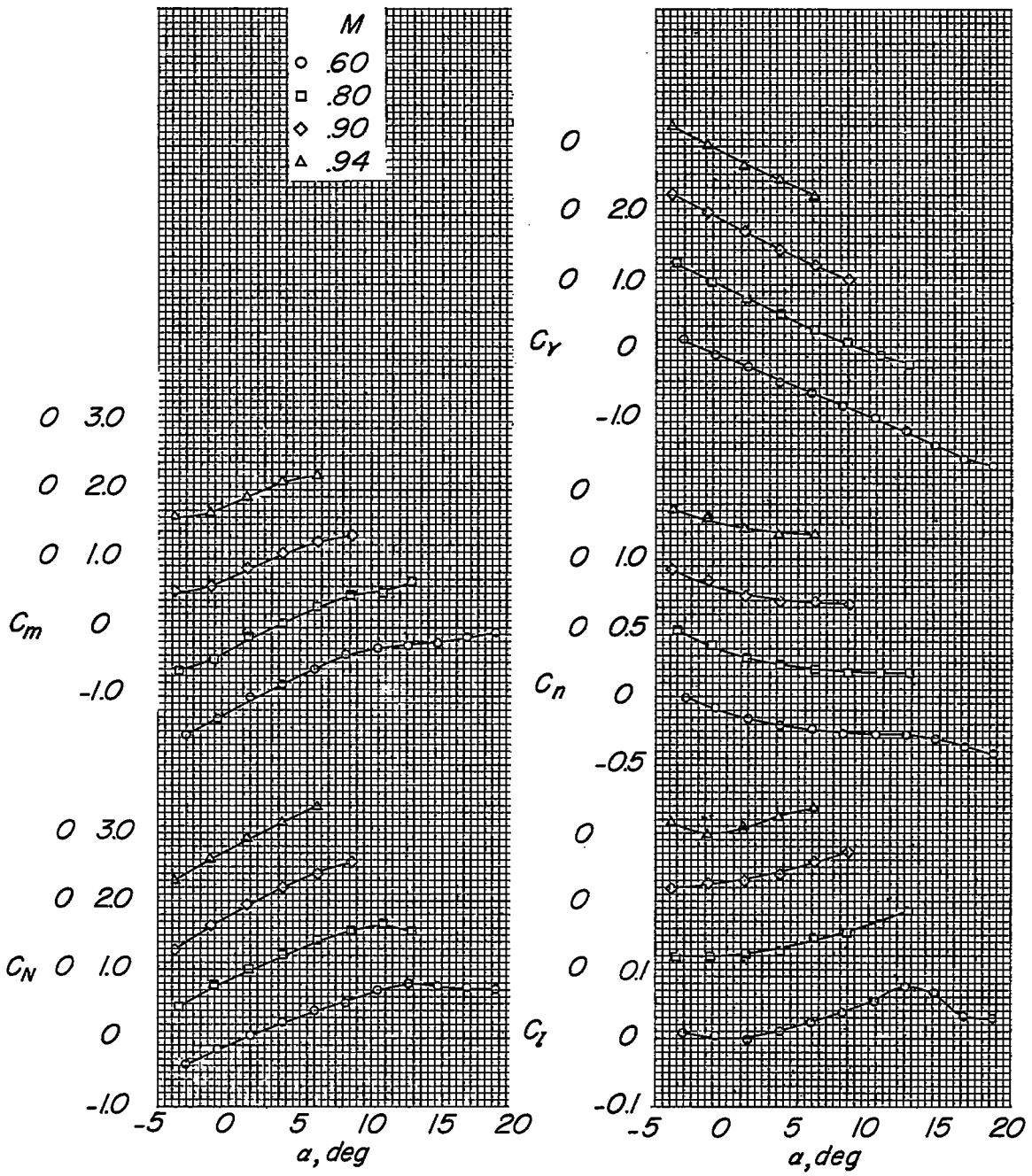

(c) x/c = 0.13.

Figure 9.- Continued.

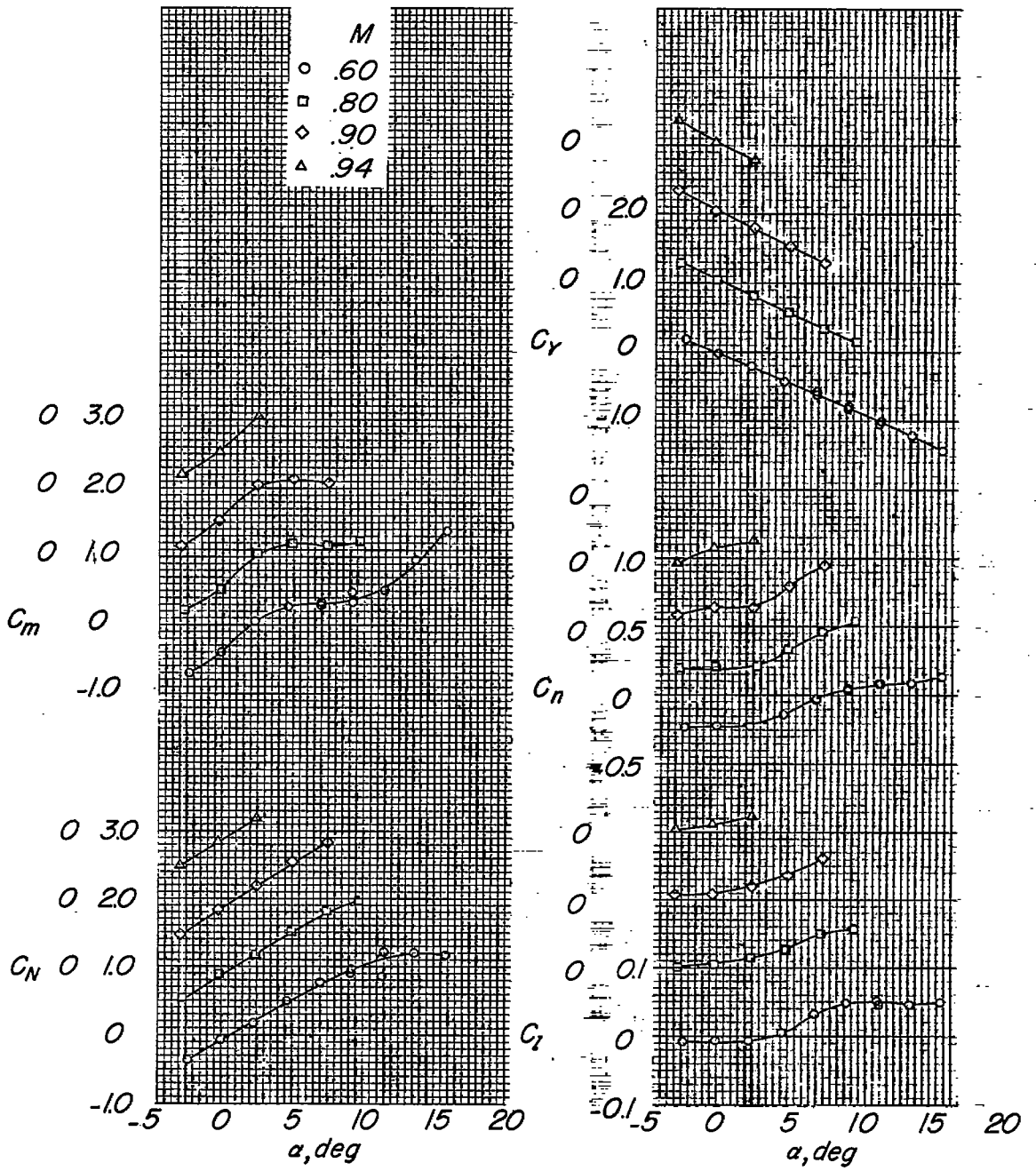

(d) x/c = -0.10.

Figure 9.- Continued.

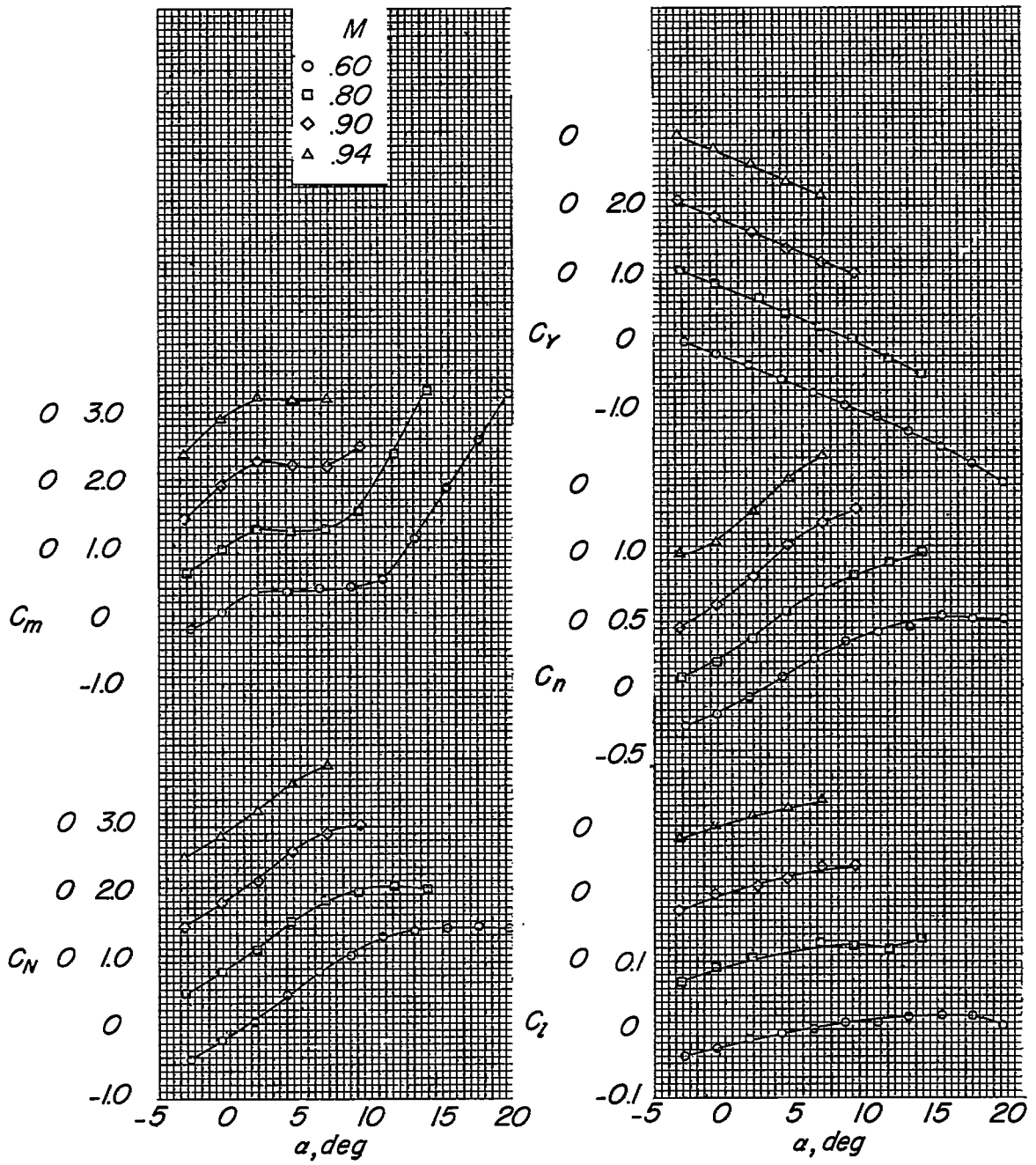

(e) x/c = -0.25.

Figure 9.- Continued.

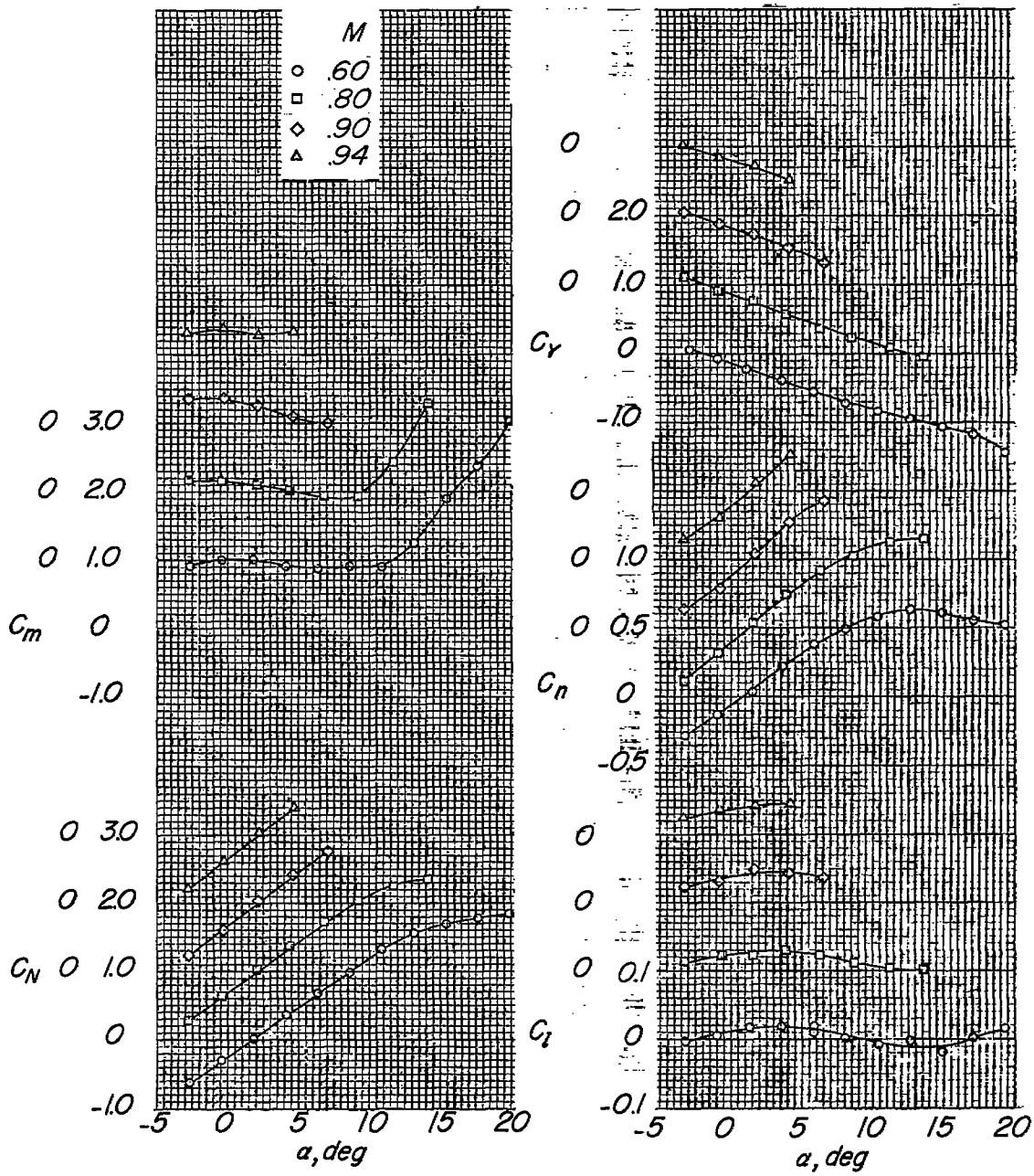

(f) x/c = -0.44.

Figure 9.- Continued.

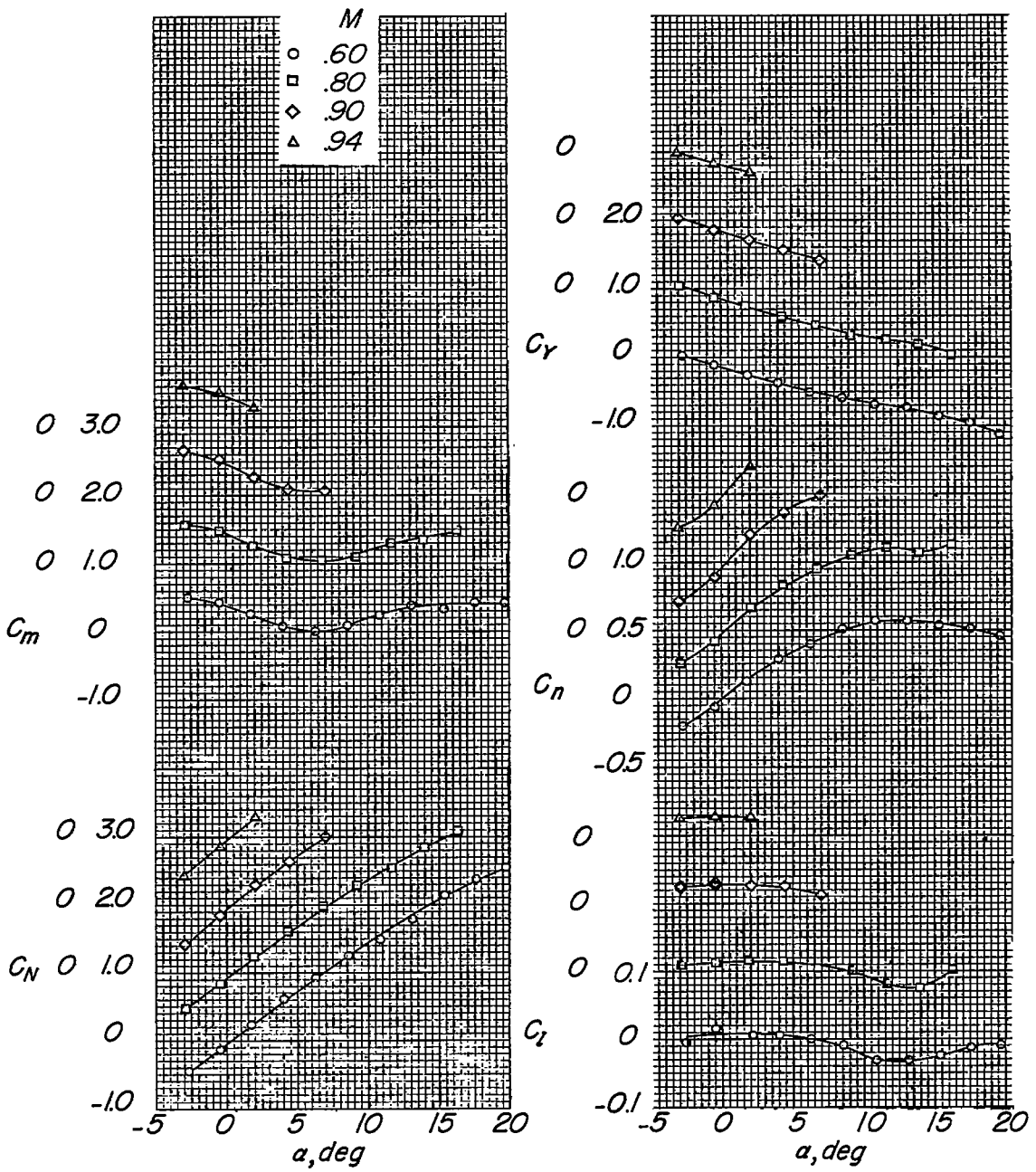

(g) x/c = -0.58.

Figure 9.- Continued.

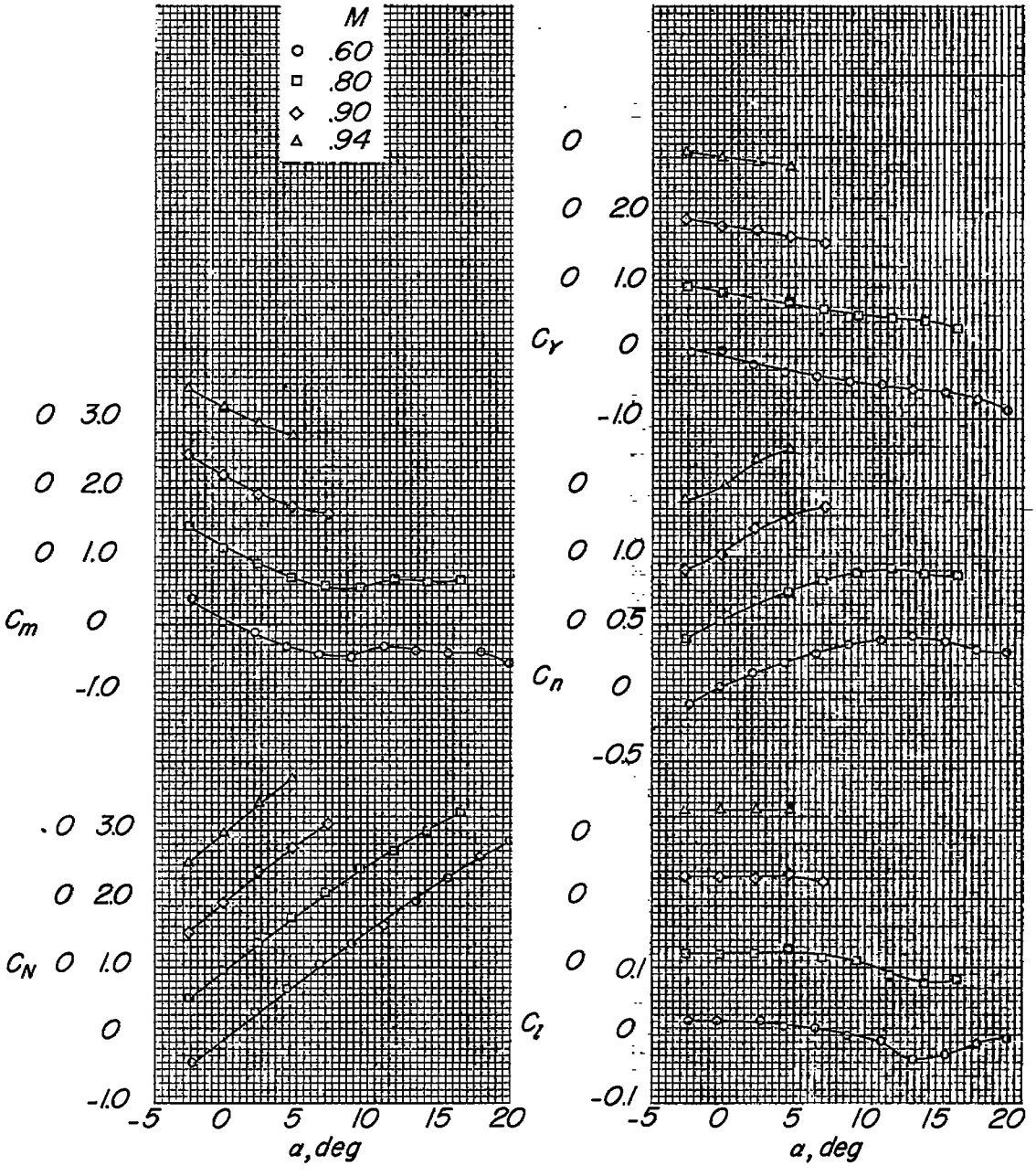

(h) x/c = -0.74.

Figure 9.- Continued.

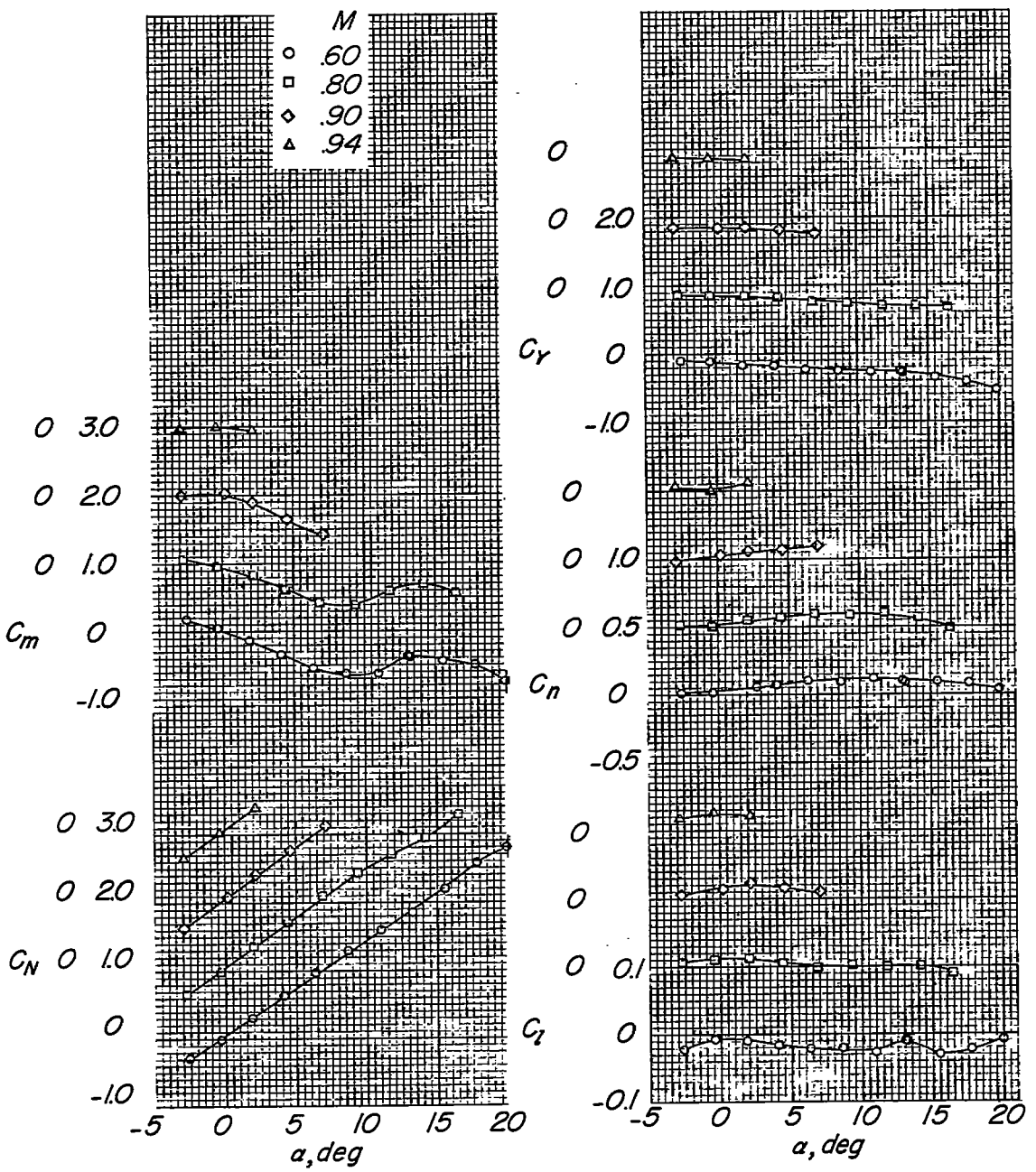

(i) x/c = 1.11.

Figure 9.- Concluded.

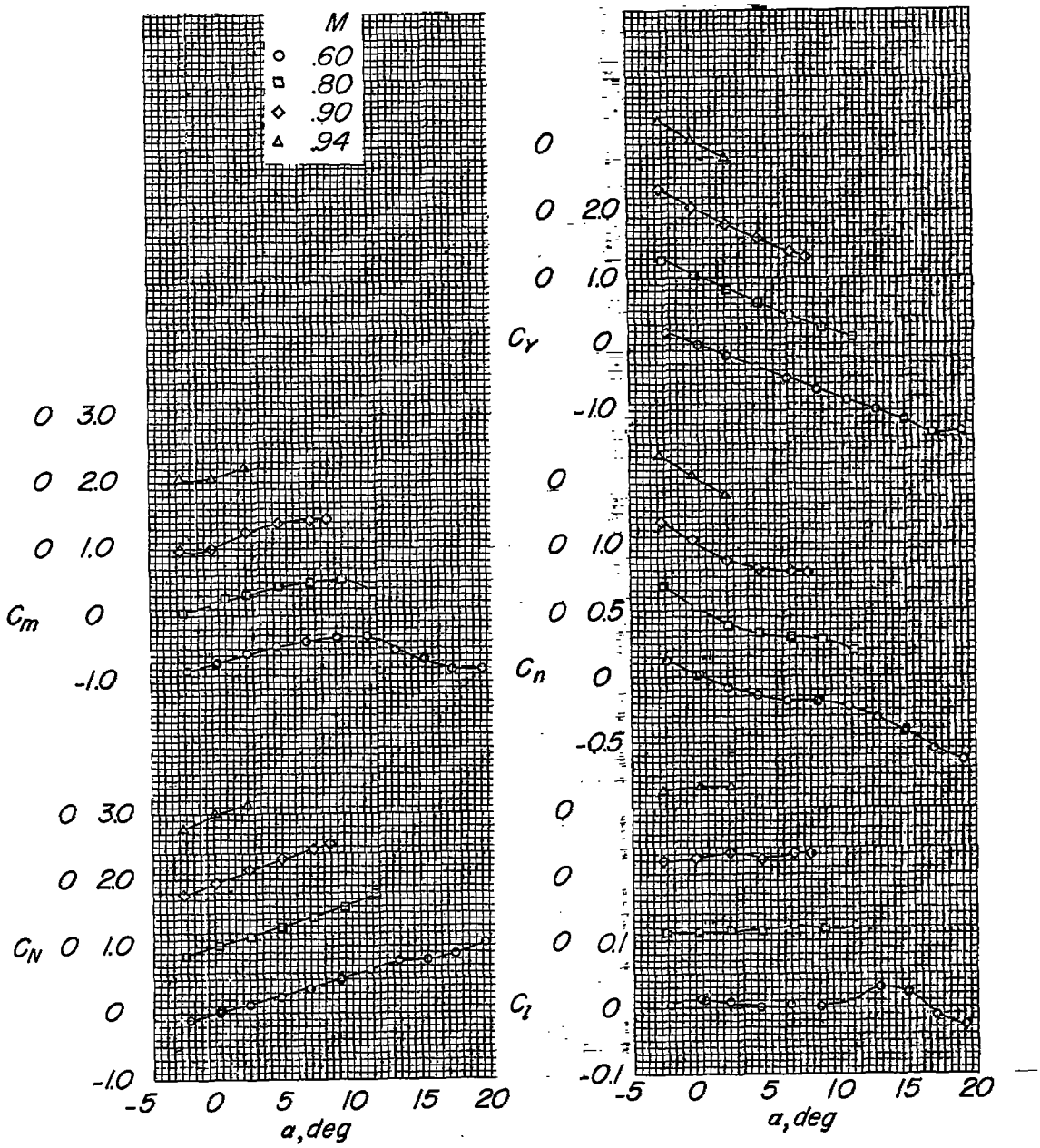

(a) x/c = 0.29.

Figure 10.- Missile aerodynamic characteristics in the presence of the wing-fuselage combination for various Mach numbers and chordwise locations (pylon removed). z/c = -0.16; $\beta_m = 0^\circ$; $\beta_A = 0^\circ$.

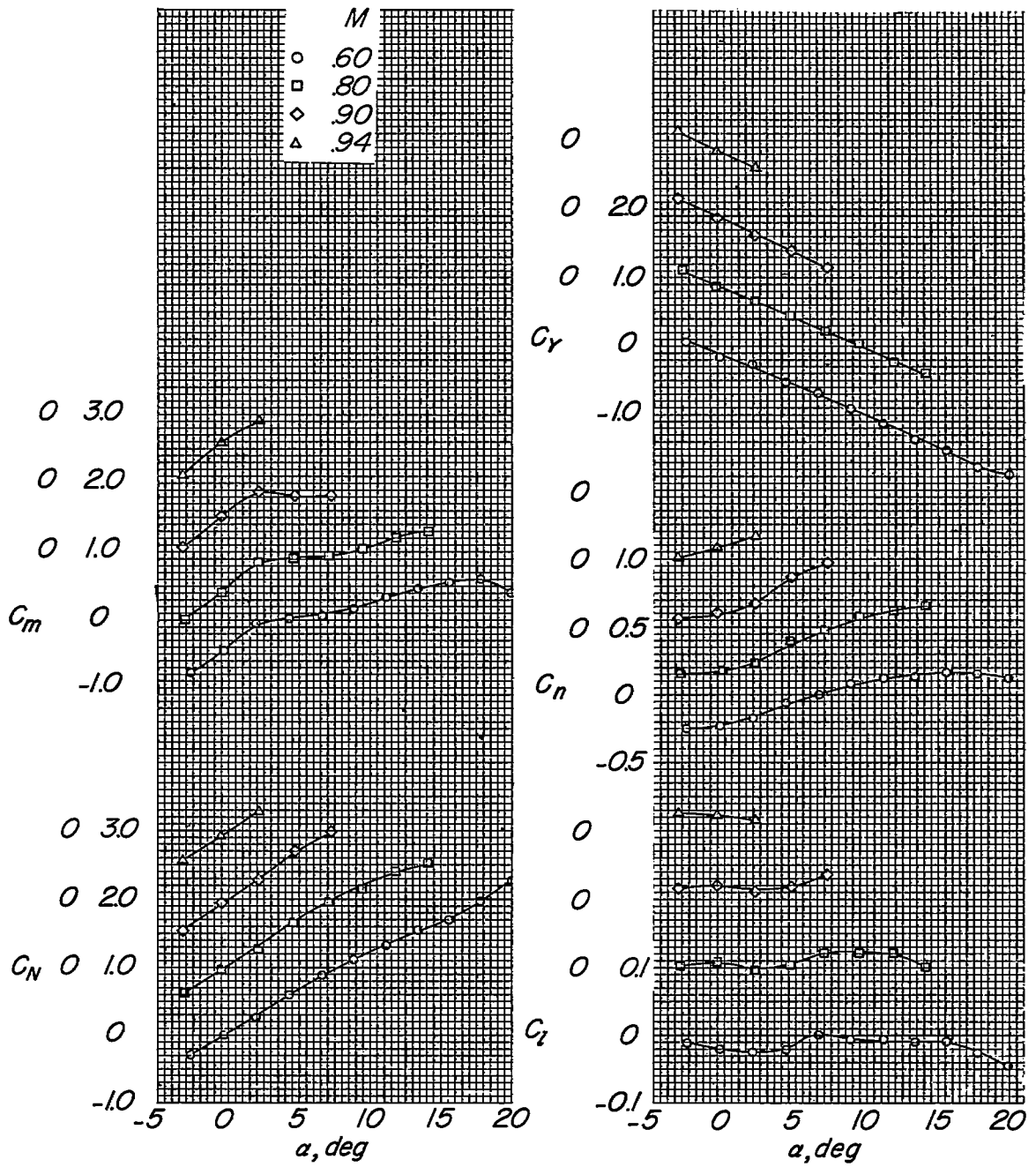

(b) x/c = -0.10.

Figure 10.- Continued.

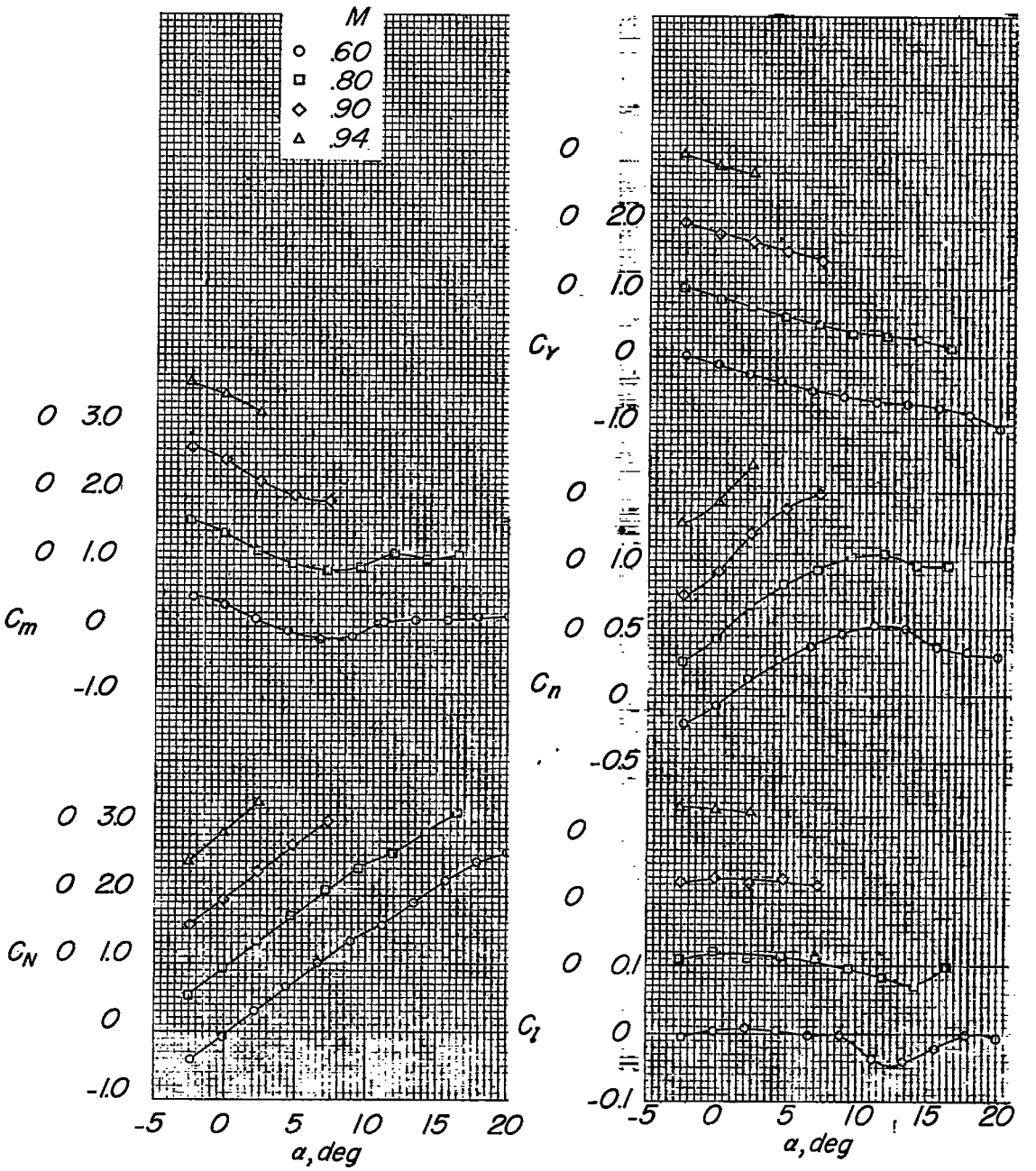

(c) x/c = -0.58.

Figure 10.- Concluded.

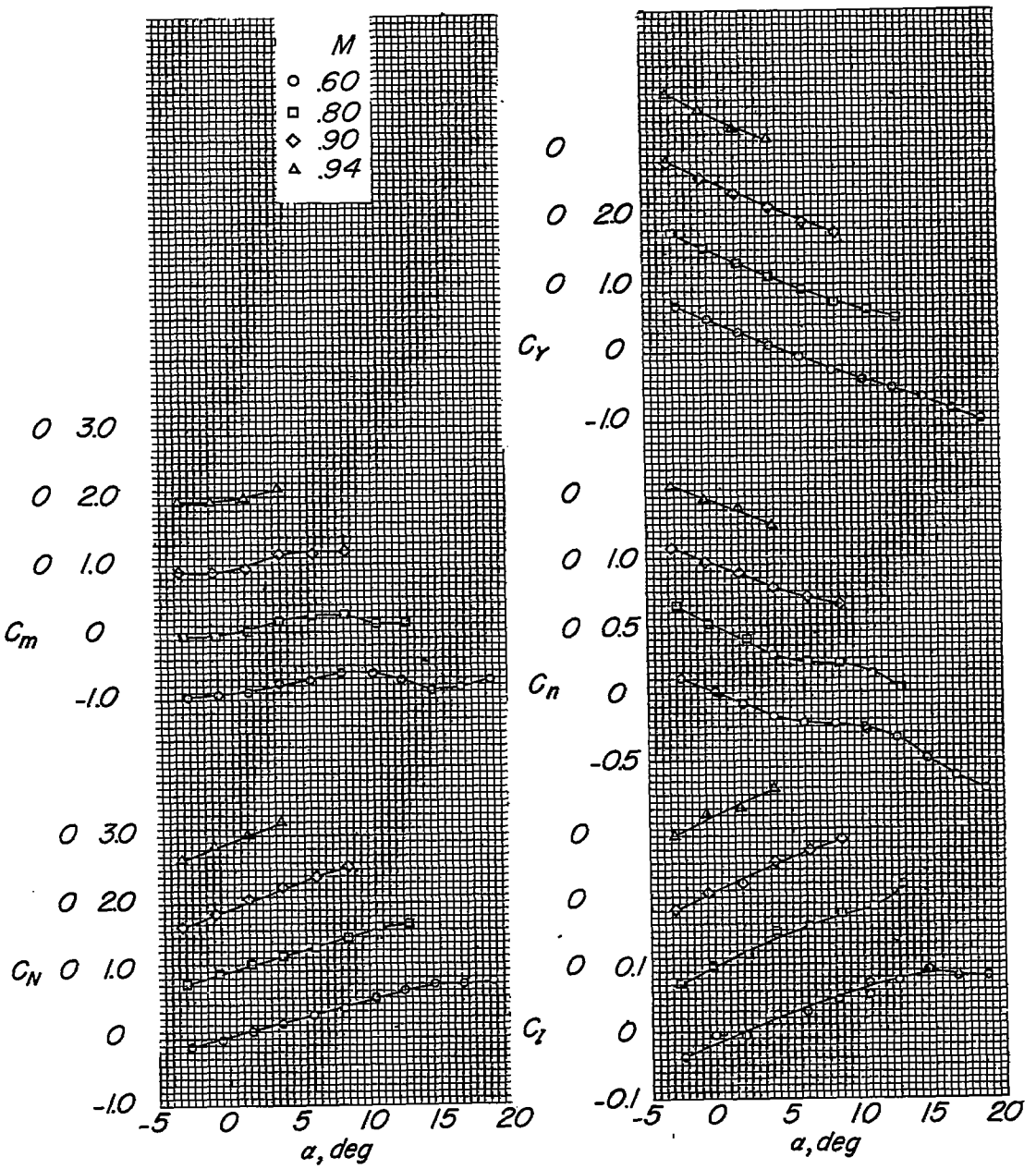

(a) $\beta_m = -4^\circ$; $\beta_A = 0^\circ$.

Figure 11.- Effects of sideslip on the missile aerodynamic characteristics in the presence of the wing-fuselage-pylon combination for various Mach numbers. z/c = -0.16; x/c = 0.29.

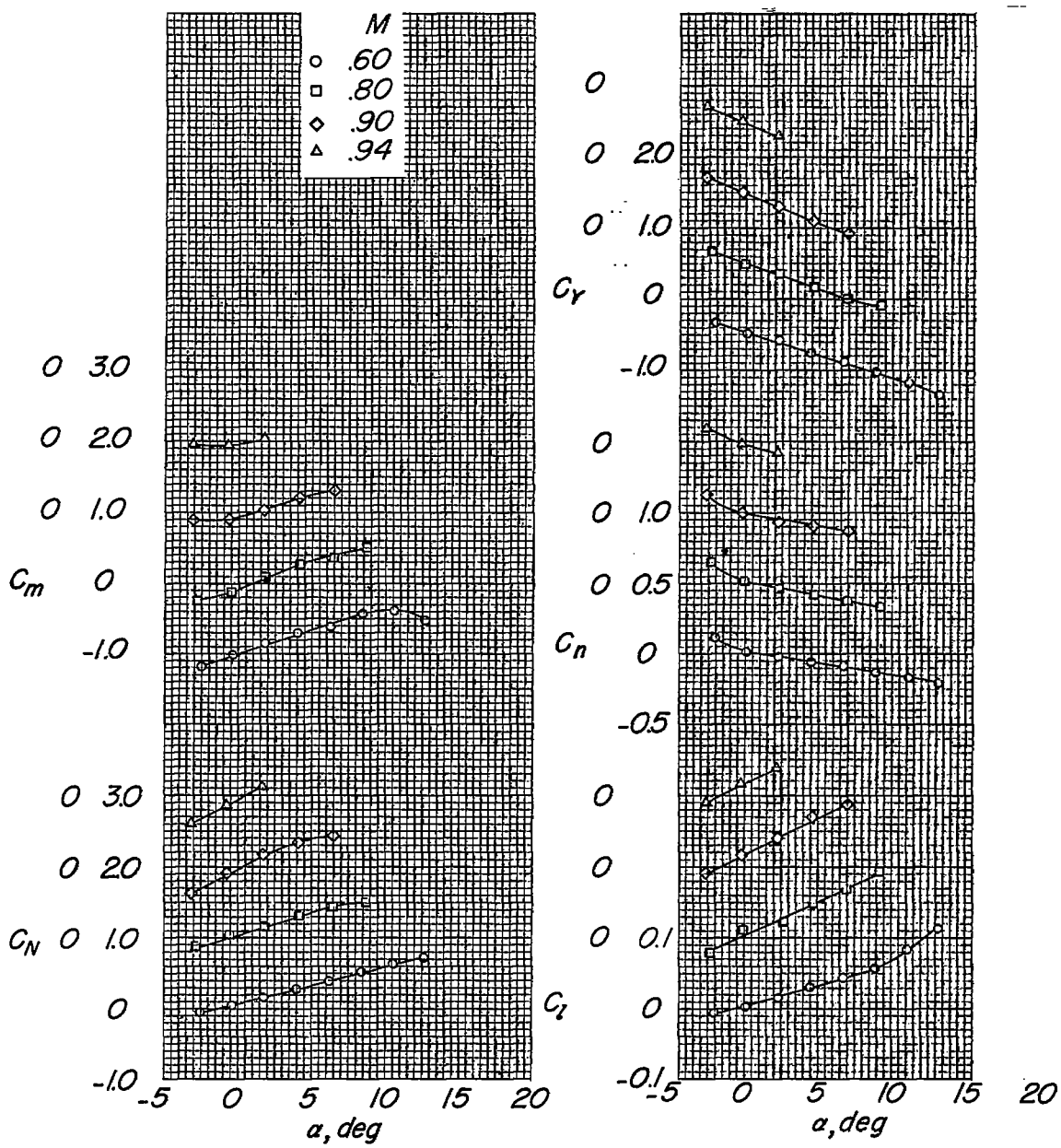

(b) $\beta_m = 4^\circ$; $\beta_A = 0^\circ$.

Figure 11.- Continued.

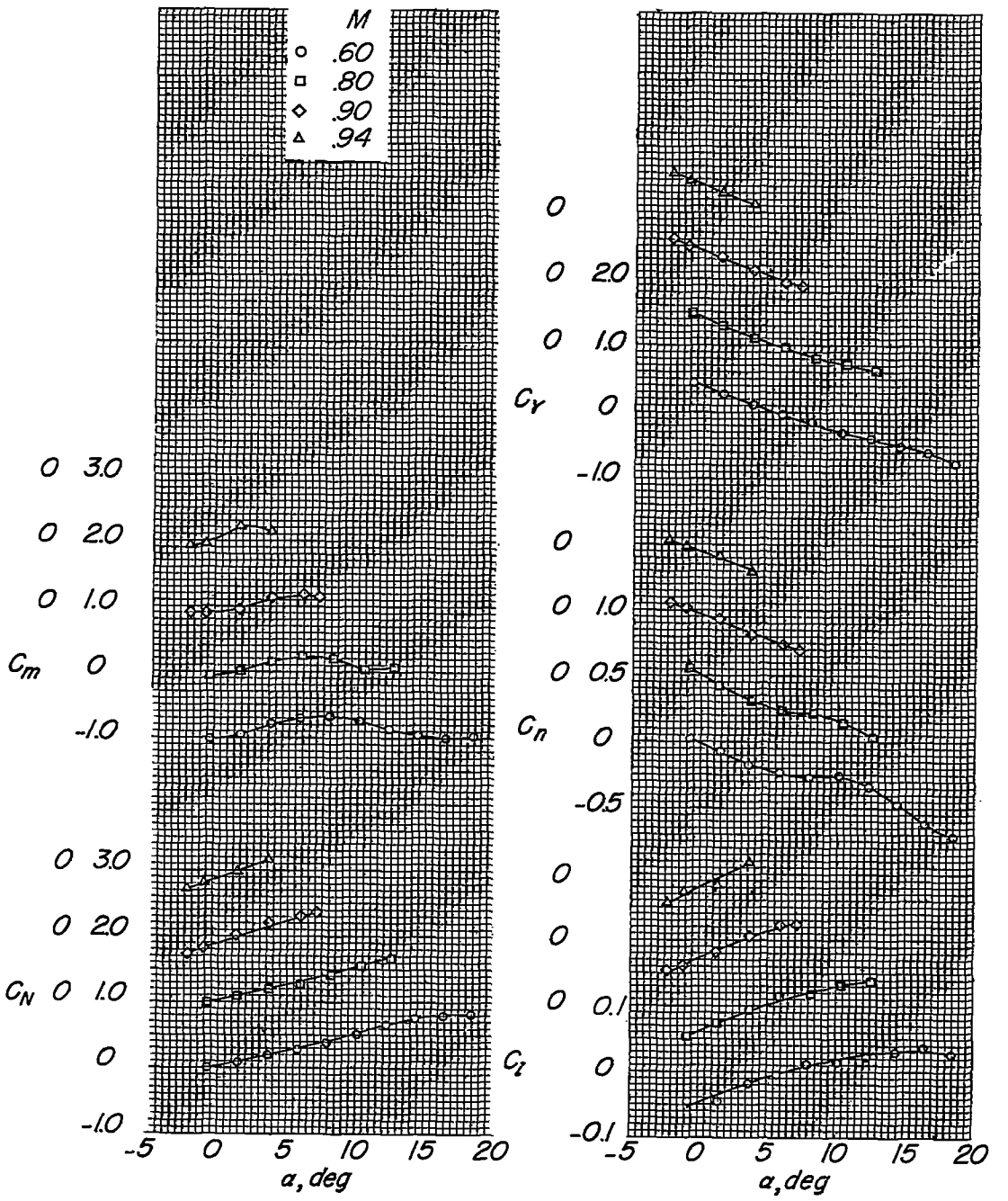

(c) $\beta_A = -4^\circ$; $\beta_m = 0^\circ$.

Figure 11.- Continued.

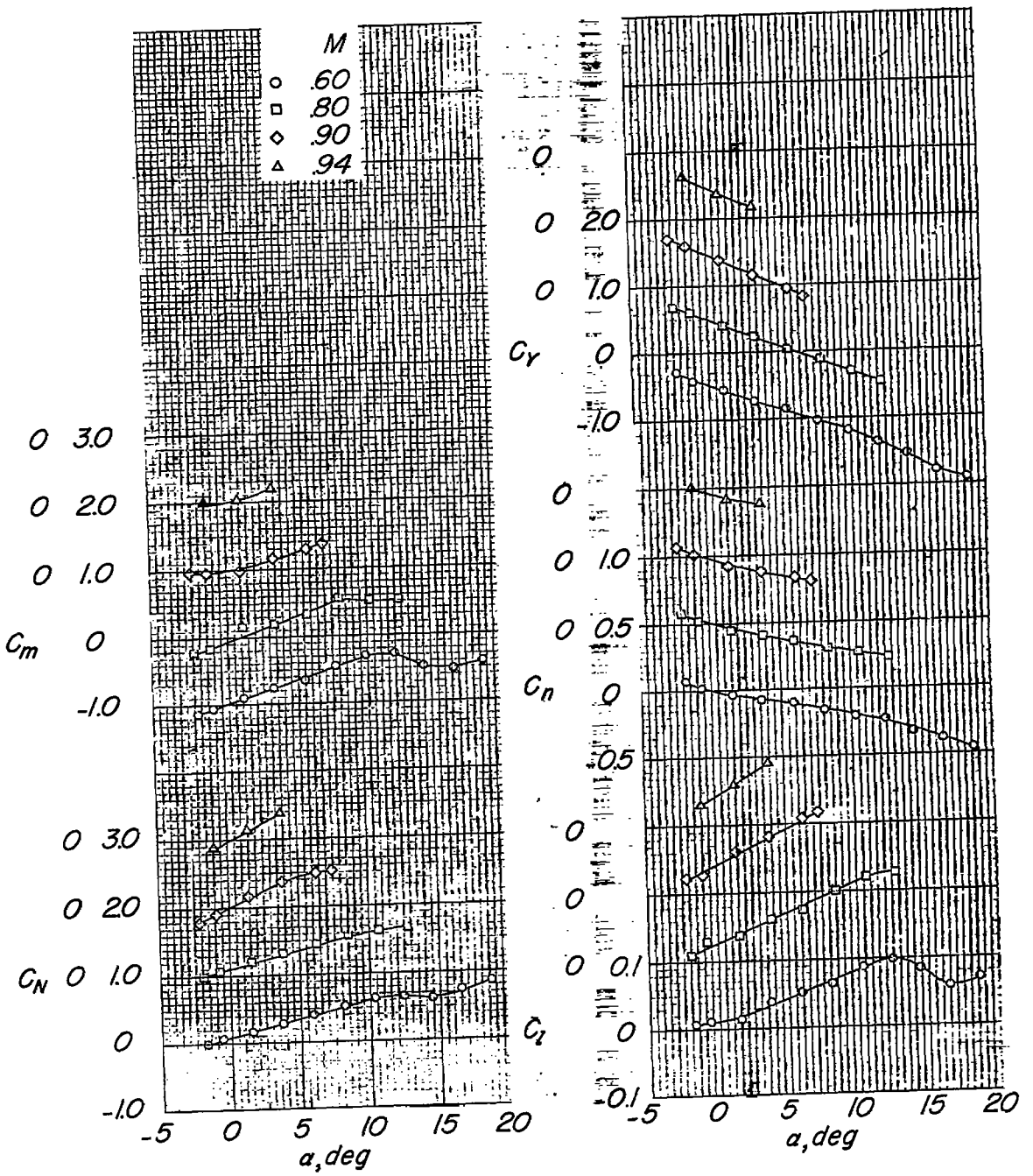

(d) $\beta_A = 4^\circ$; $\beta_m = 0^\circ$.

Figure 11.- Concluded.

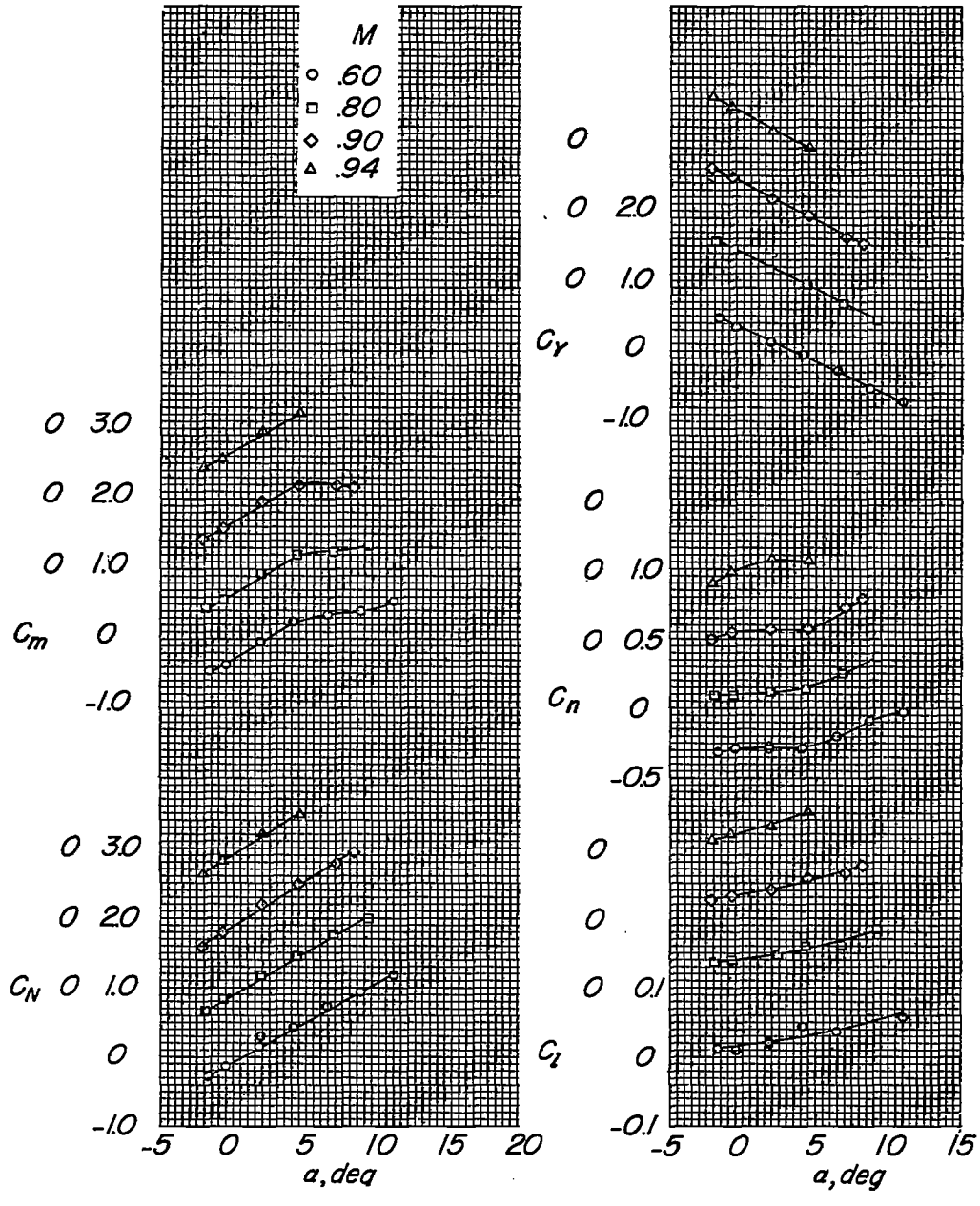

(a) $\beta_m = -4^\circ$; $\beta_A = 0^\circ$.

Figure 12.- Effects of sideslip on the missile aerodynamic forces and moments in the presence of the wing-fuselage-pylon combination for various Mach numbers. z/c = -0.16; x/c = -0.10.

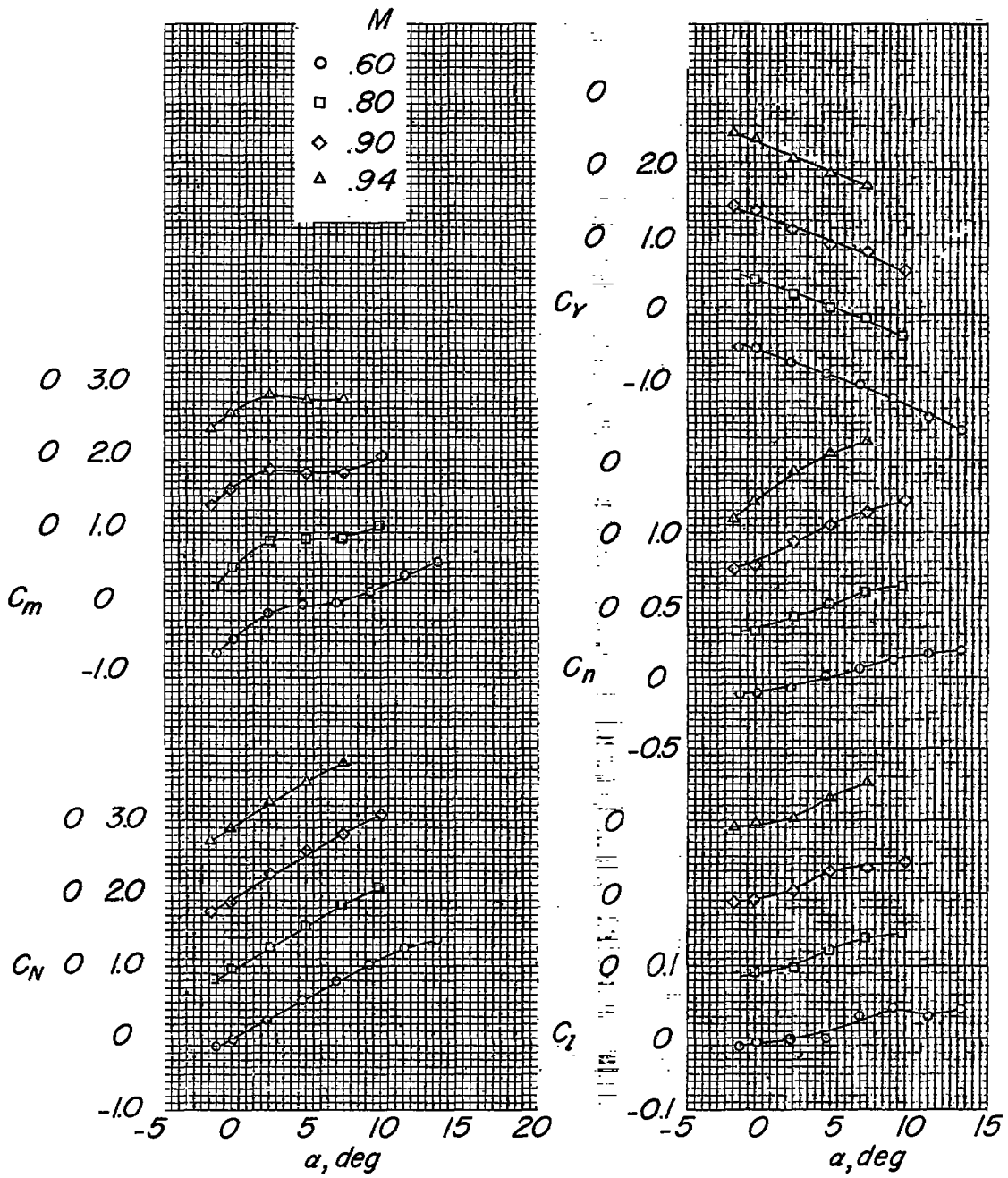

(b) $\beta_m = 4^\circ$; $\beta_A = 0^\circ$.

Figure 12.- Continued.

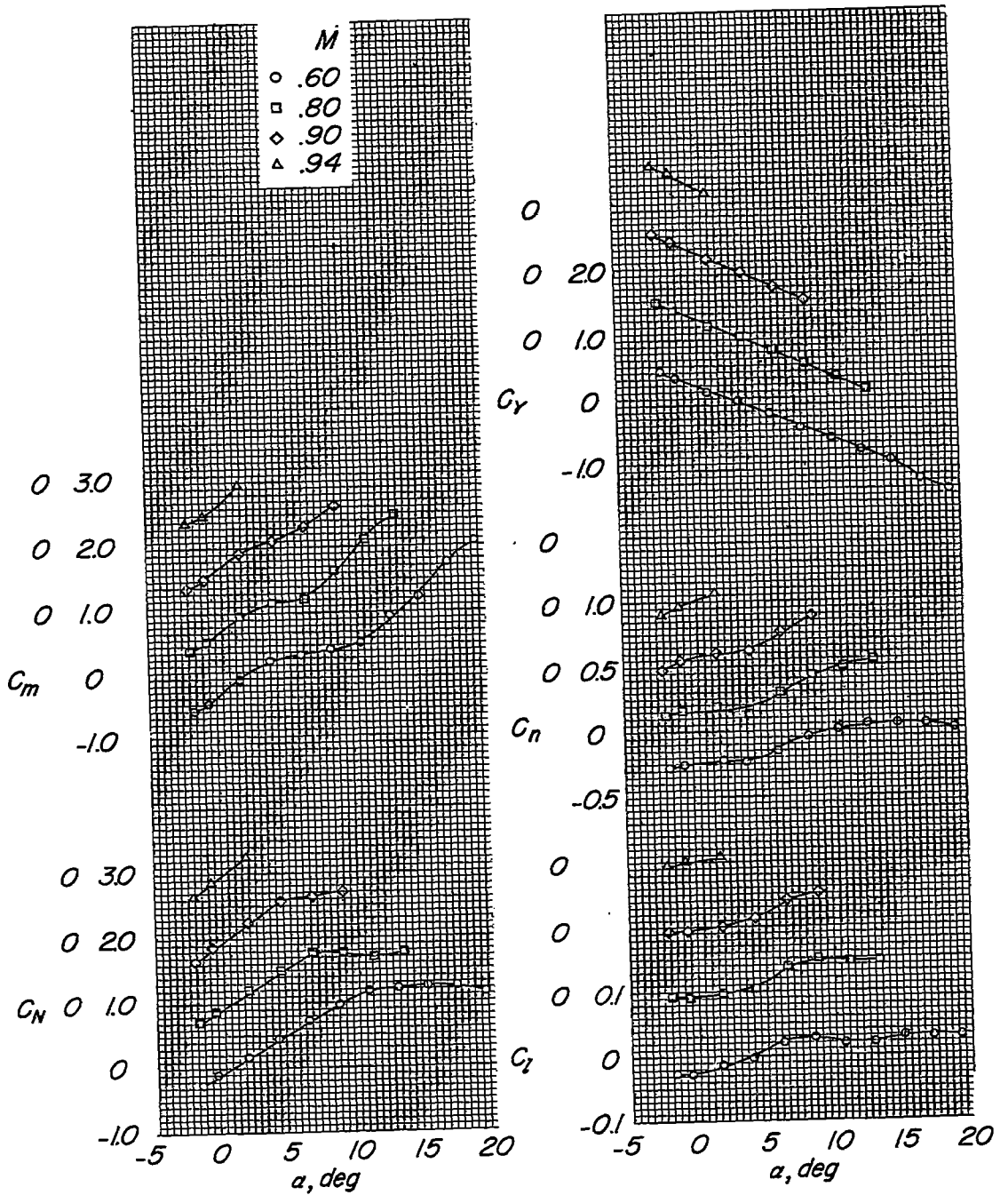

(c) $\beta_A = -4^\circ$; $\beta_m = 0^\circ$.

Figure 12.- Continued.

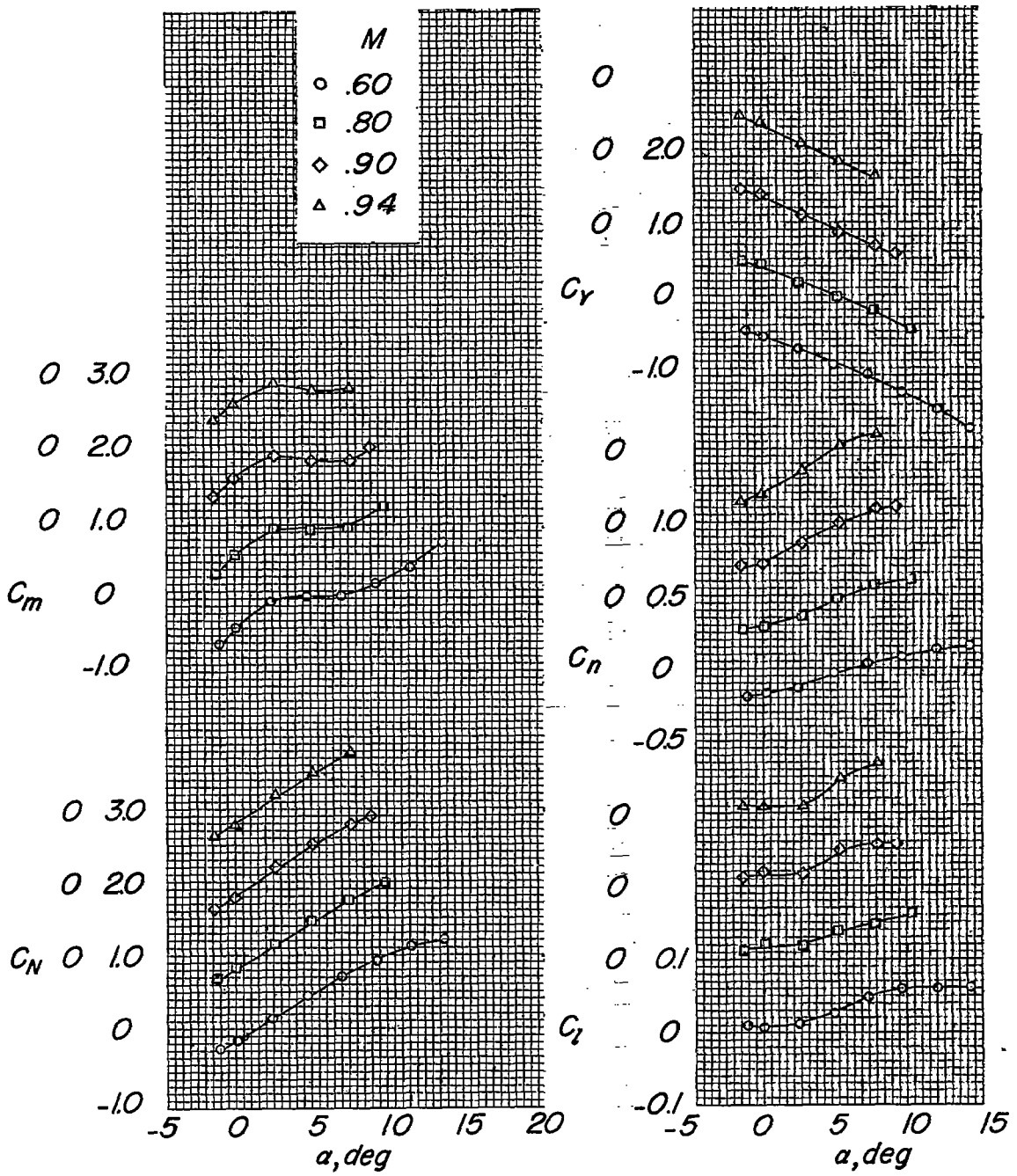

(d) $\beta_A = 4^\circ$; $\beta_m = 0^\circ$.

Figure 12.- Concluded.

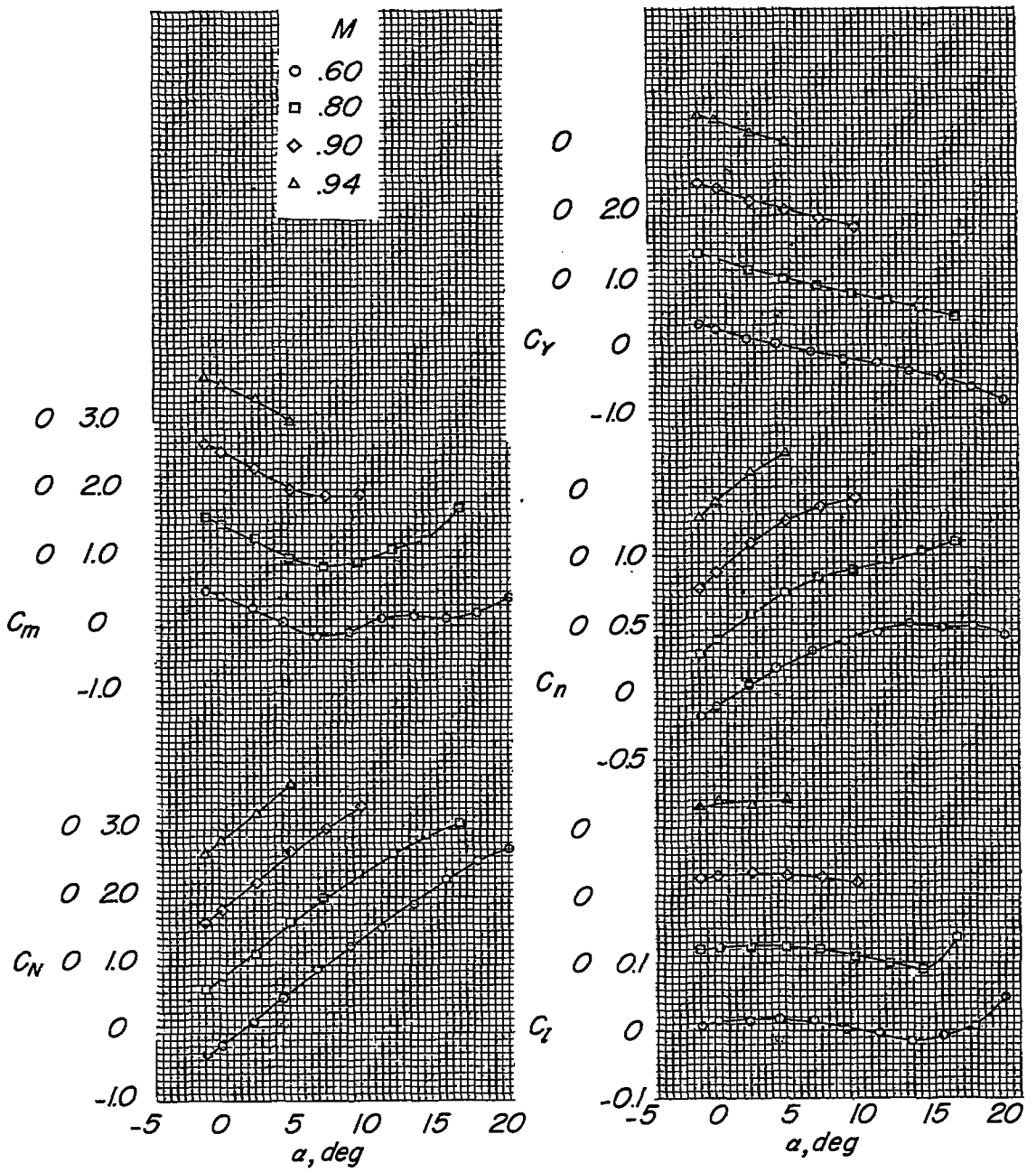

(a) $\beta_m = -4^\circ$; $\beta_A = 0^\circ$.

Figure 13.- Effect of sideslip on the missile aerodynamic forces and moments in the presence of the wing-fuselage-pylon combination at various Mach numbers. z/c = -0.16; x/c = -0.58.

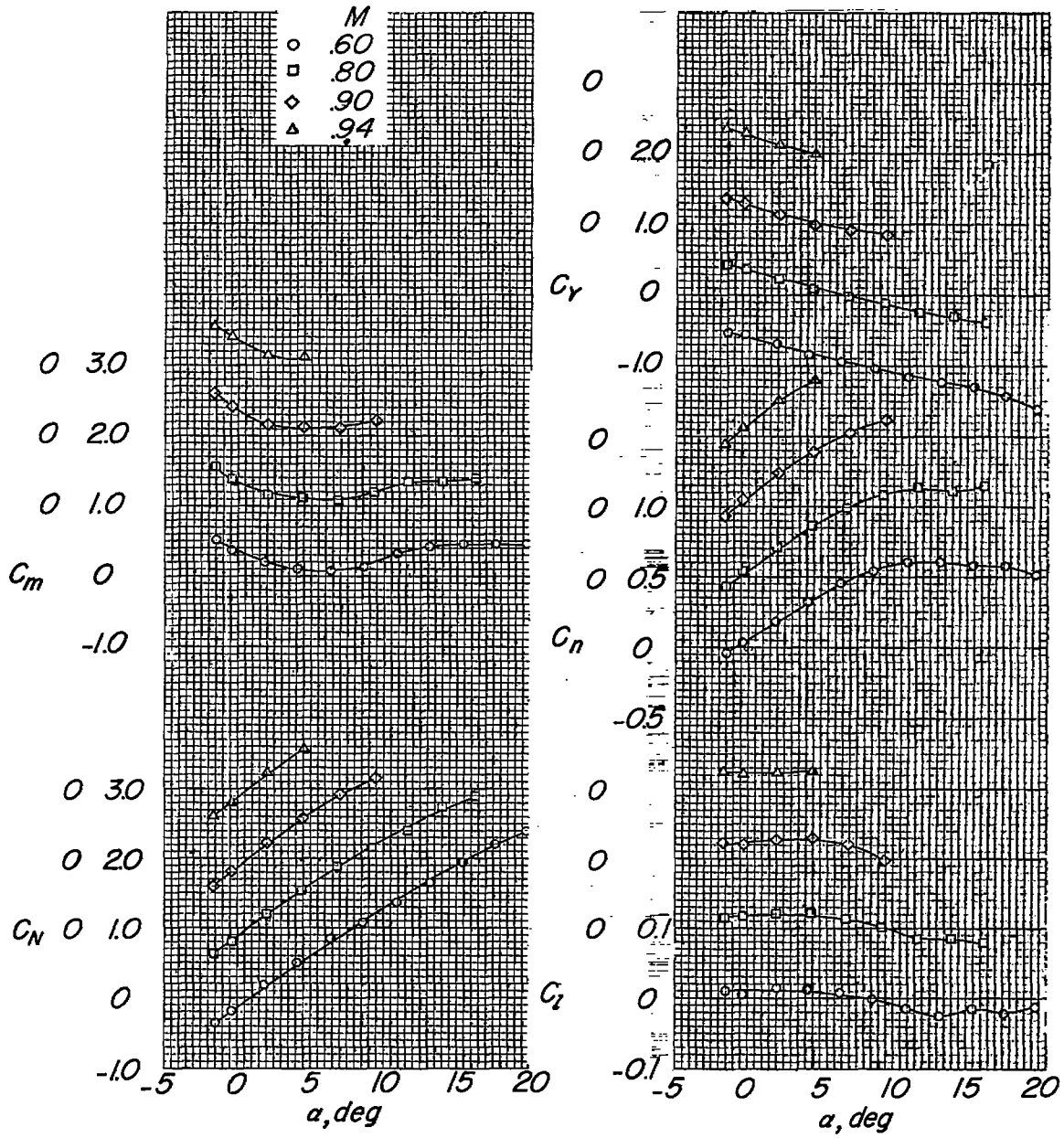

(b) $\beta_m = 4^\circ$; $\beta_A = 0^\circ$.

Figure 13.- Continued.

[redacted]

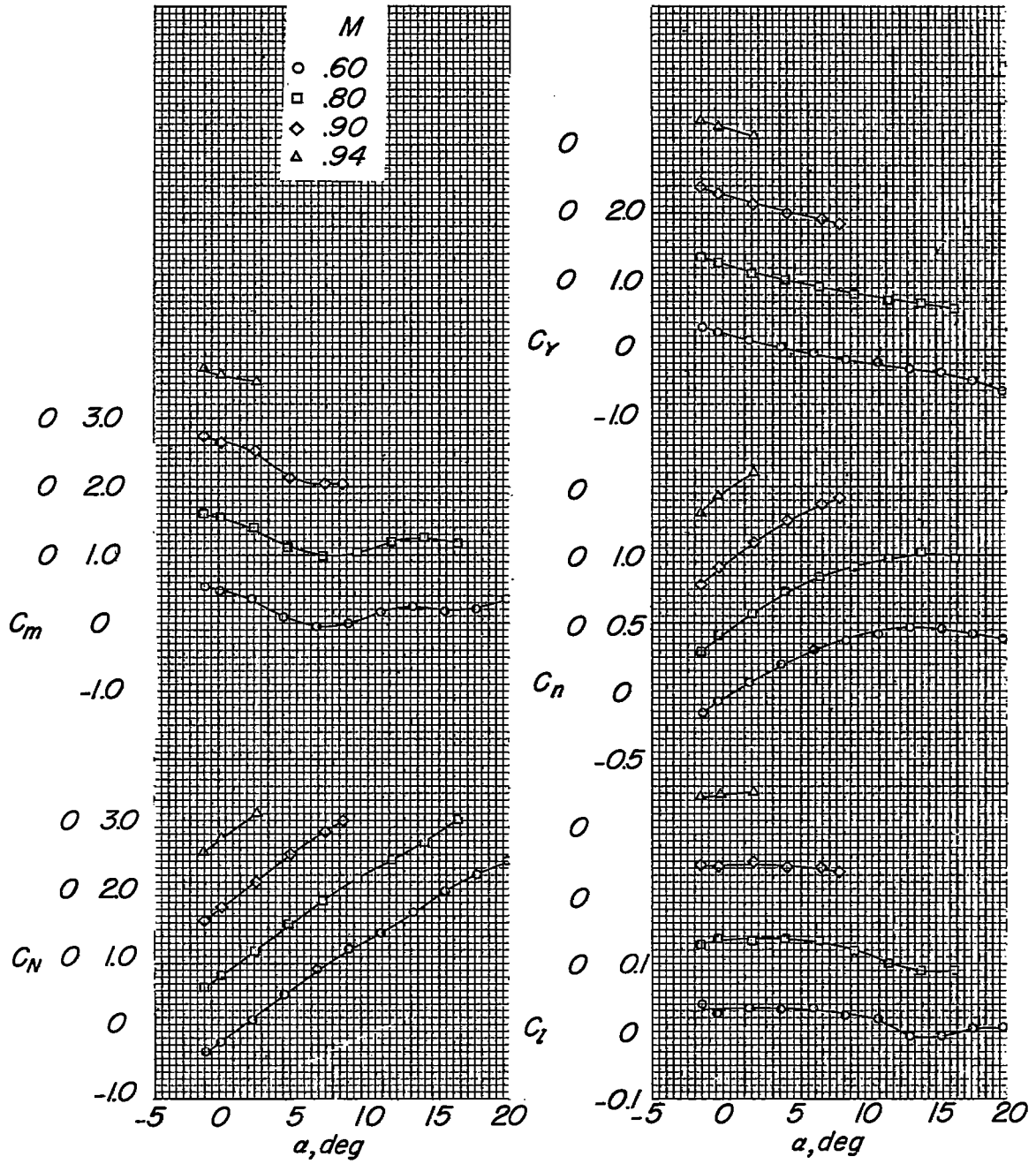

(c) $\beta_A = -4^\circ$; $\beta_m = 0^\circ$.

Figure 13.- Continued.

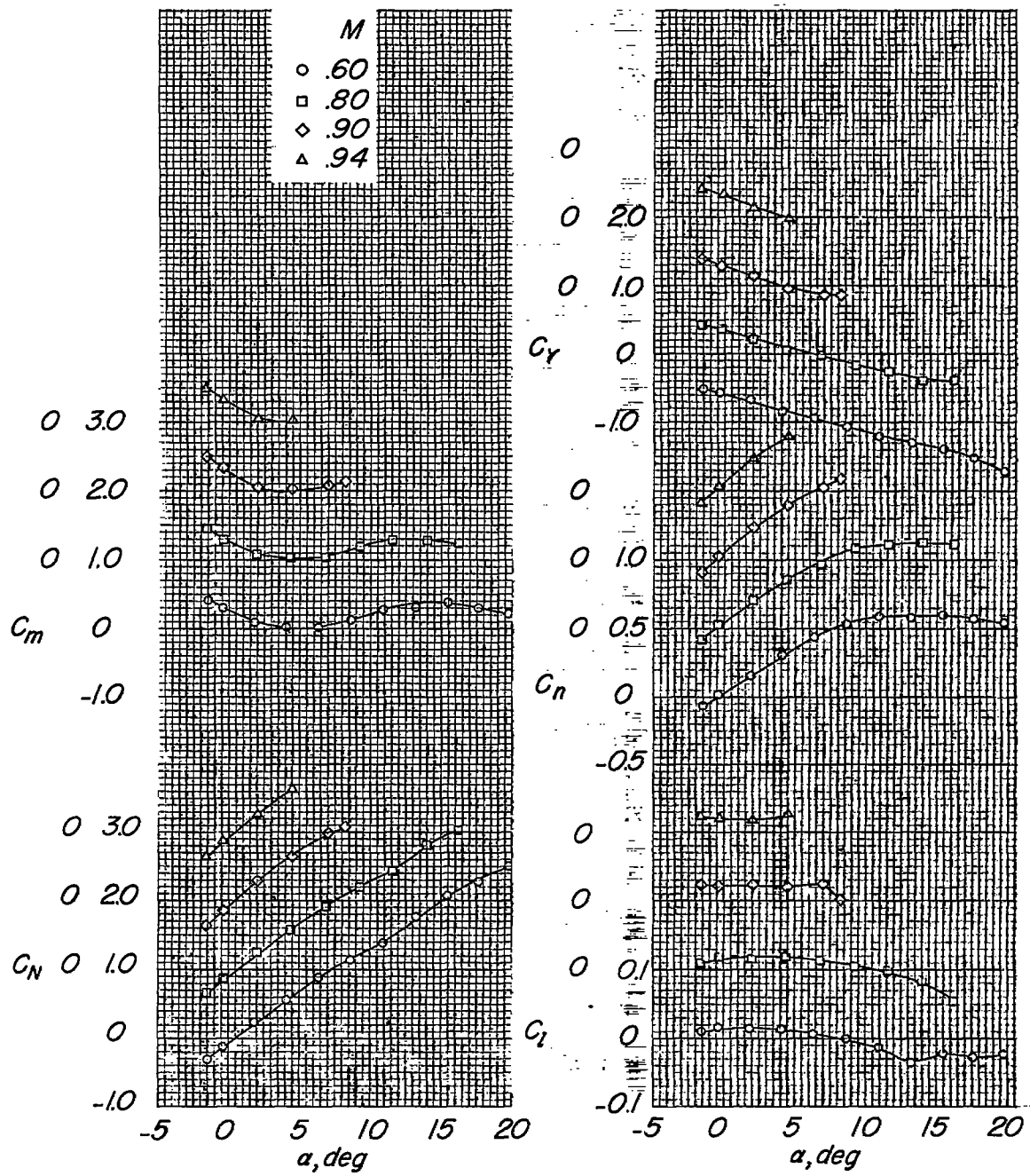

(d) $\beta_A = 4^\circ$; $\beta_m = 0^\circ$.

Figure 13.- Concluded.

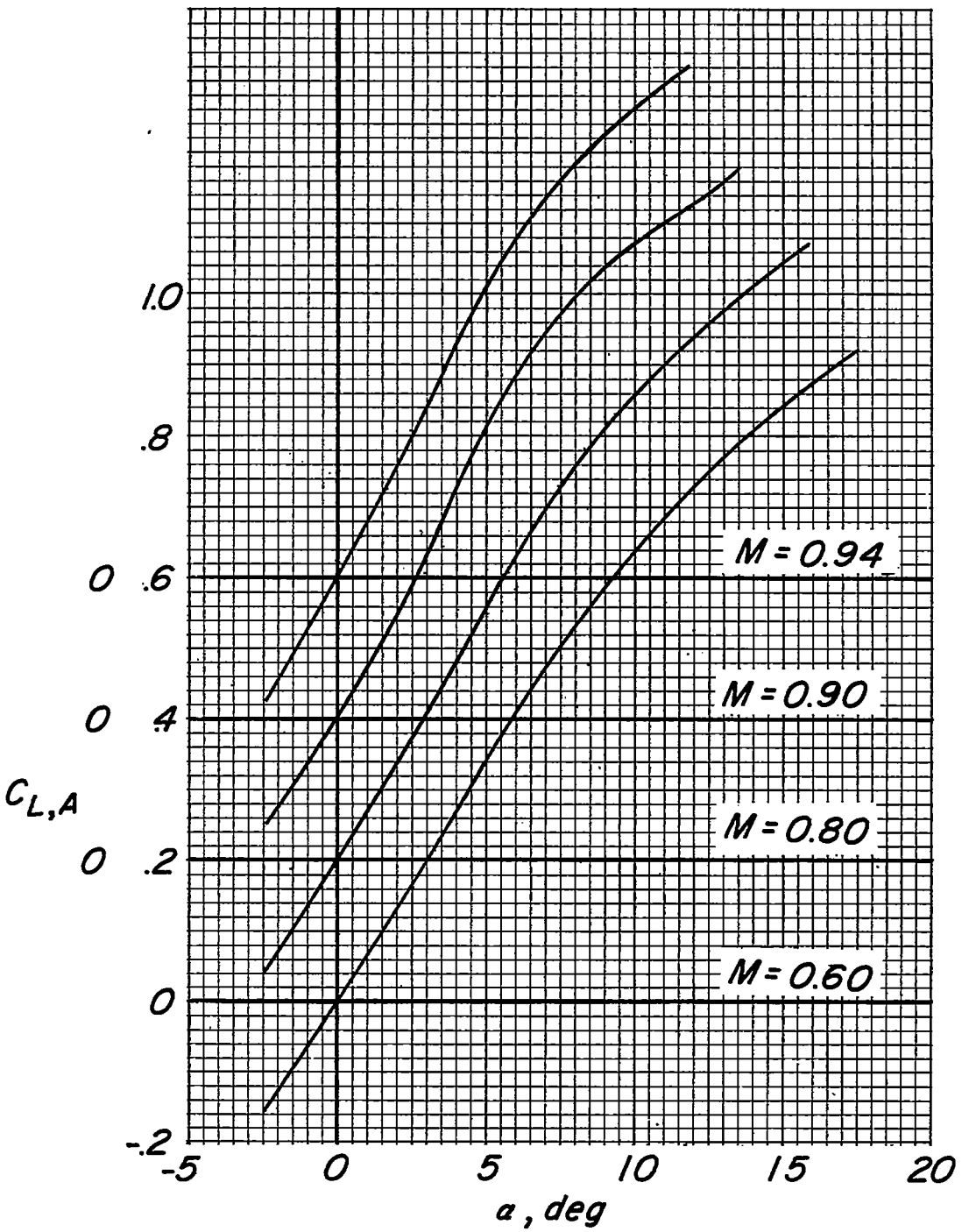

Figure 14.- Lift characteristics of the isolated wing-fuselage combination.